

AD-A056 890

ILLINOIS UNIV AT URBANA-CHAMPAIGN COORDINATED SCIENCE LAB F/G 9/5
TIME DOMAIN ANALYSIS OF SAW FILTERS.(U)

MAY 77 C M PANASIK

DAAB07-72-C-0259

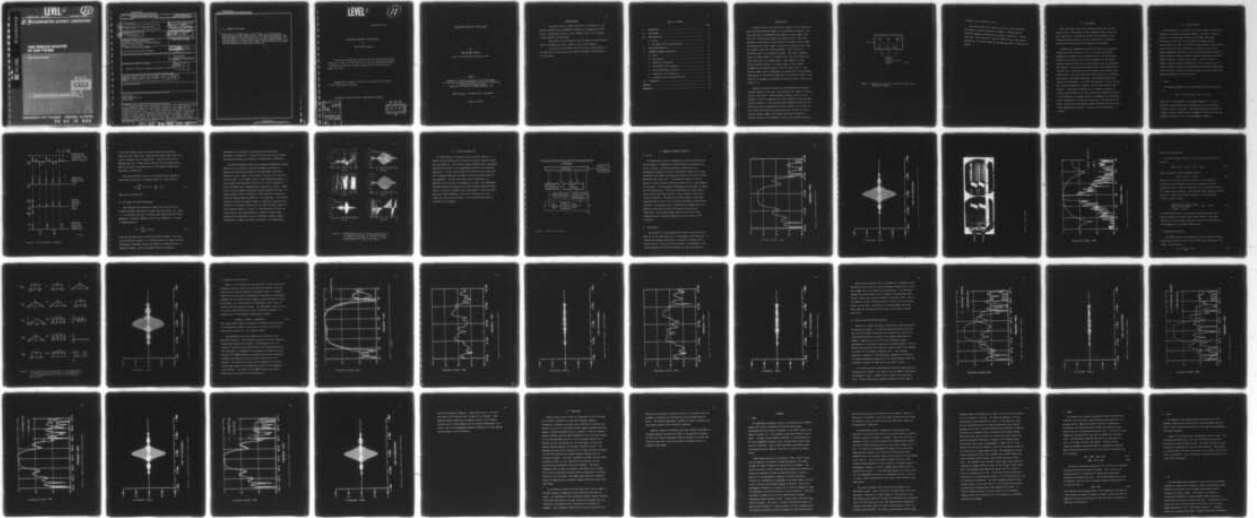
UNCLASSIFIED

R-781

NL

1 OF 1

AD
A056890



END
DATE
FILMED
9-78
DDC

LEVEL II



REPORT R-781 MAY, 1977

UILU-ENG 77-2228

CSL COORDINATED SCIENCE LABORATORY

AD A 056890

**TIME DOMAIN ANALYSIS
OF SAW FILTERS**

CARL MICHAEL PANASIK

AD NU.
DDC FILE COPY

DDC
RECEIVED
AUG 2 1978
D

APPROVED FOR PUBLIC RELEASE. DISTRIBUTION UNLIMITED.

UNIVERSITY OF ILLINOIS - URBANA, ILLINOIS

78 07 10 038

UNCLASSIFIED

SECURITY CLASSIFICATION OF THIS PAGE (When Data Entered)

REPORT DOCUMENTATION PAGE		READ INSTRUCTIONS BEFORE COMPLETING FORM
1. REPORT NUMBER	2. GOVT ACCESSION NO.	3. RECIPIENT'S CATALOG NUMBER
4. TITLE (and Subtitle) 6 TIME DOMAIN ANALYSIS OF SAW FILTERS		5. TYPE OF REPORT & PERIOD COVERED 9 Technical Report
7. AUTHOR(s) 10 Carl Michael Panasik		6. PERFORMING ORG. REPORT NUMBER R-781; UILU-ENG 77-2228 CONTRACT OR GRANT NUMBER(S) 15 DAAR-77-72-C-0259; F33615-75-C-1291
9. PERFORMING ORGANIZATION NAME AND ADDRESS Coordinated Science Laboratory University of Illinois at Urbana-Champaign Urbana, Illinois 61801		10. PROGRAM ELEMENT, PROJECT, TASK AREA & WORK UNIT NUMBERS
11. CONTROLLING OFFICE NAME AND ADDRESS Joint Services Electronics Program		12. REPORT DATE 11 May 77 13. NUMBER OF PAGES 49
14. MONITORING AGENCY NAME & ADDRESS (if different from Controlling Office)		15. SECURITY CLASS. (of this report) UNCLASSIFIED 15a. DECLASSIFICATION/DOWNGRADING SCHEDULE
16. DISTRIBUTION STATEMENT (of this Report) Approved for public release; distribution unlimited 12 56 p.		
17. DISTRIBUTION STATEMENT (of the abstract entered in Block 20, if different from Report) 14 R-781, UILU-ENG-77-2228		
18. SUPPLEMENTARY NOTES		
19. KEY WORDS (Continue on reverse side if necessary and identify by block number) SAW Filters Time Domain Analysis Equalization		
20. ABSTRACT (Continue on reverse side if necessary and identify by block number) A Surface Acoustic Wave (SAW) device consists of two transducers with interleaved aluminum fingers on a piezoelectric substrate. The input transducer is implemented with fingers of equal length, while the output transducer has fingers with varied overlap. The filter operates by electrically exciting the input transducer which through the piezoelectric effect causes a surface wave along with other modes to propagate toward the output transducer. There the wave is transformed back into an electrical signal. The output transducer works in a manner similar to a digital filter and can be modeled as a tapped		

UNCLASSIFIED

SECURITY CLASSIFICATION OF THIS PAGE(When Data Entered)

20. ABSTRACT (continued)

delay line of N fingers where 1) each finger is a delta function generator-detector of surface waves, 2) the constant propagation time between fingers is the unit delay time t , 3) the variable finger overlap (apodization) is proportional to an attenuator weight W_k^t and 4) the relative direction of overlap with respect to the direction of propagation determines the relative sign of that tap.

UNCLASSIFIED

SECURITY CLASSIFICATION OF THIS PAGE(When Data Entered)

LEVEL II



UILU-ENG 77-2228

TIME DOMAIN ANALYSIS OF SAW FILTERS

by

Carl Michael Panasik

This work was supported in part by the Joint Services Electronics Program (U.S. Army, U.S. Navy and U.S. Air Force) under Contract DAAB-07-72-C-0259 and in part by the United States Air Force under Contract F33615-75-C-1291.

Reproduction in whole or in part is permitted for any purpose of the United States Government.

Approved for public release. Distribution unlimited.

ACCESSION FOR	
DTIC	White Section <input checked="" type="checkbox"/>
DDC	Ordn Section <input type="checkbox"/>
UNANNOUNCED	<input type="checkbox"/>
JUSTIFICATION.....	
BY.....	
DISTRIBUTION/AVAILABILITY CODES	
Dist.	AVAIL. and/or SPECIAL
A	

DDC
RECEIVED
AUG 2 1978
D

TIME DOMAIN ANALYSIS OF SAW FILTERS

BY

CARL MICHAEL PANASIK

B.E.E., Cleveland State University, 1974

THESIS

Submitted in partial fulfillment of the requirements
for the degree of Master of Science in Electrical Engineering
in the Graduate College of the
University of Illinois at Urbana-Champaign, 1977

Thesis Adviser: Professor Bill J. Hunsinger

Urbana, Illinois

ACKNOWLEDGMENT

The author wishes to thank Professor B. J. Hunsinger for his constant guidance and encouragement throughout the preparation of this thesis. The personal interest in this research shown by Dr. Hunsinger is also gratefully acknowledged.

The author is also indebted to Mr. Tom Fosha, Mr. Harold Ravlin, and Mr. Don Malocha for their technical advice and assistance.

In particular, the author would like to give special thanks to his wife, Bev, for her patience and support throughout the preparation of this thesis.

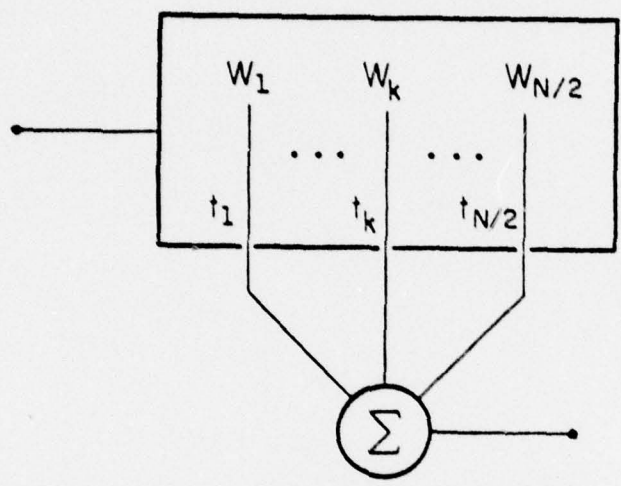
TABLE OF CONTENTS

	Page
I. INTRODUCTION	1
II. THE PROBLEM	4
III. TETAM ANALYSIS.....	5
A. Theory	5
B. Tap Weight and Delay Measurement	9
IV. TETAM IMPLEMENTATION	12
V. FREQUENCY RESPONSE CORRECTION	14
A. Device	14
B. The Approach	14
C. TETAM Data Measurement	19
D. Experimental Input Response	20
E. Output Experimental Response.....	21
F. Comparison with Theoretical	24
G. Consistent Error Equalized Response	30
VI. CONCLUSION	41
APPENDIX	43
REFERENCES	49

I. INTRODUCTION

A Surface Acoustic Wave (SAW) device consists of two transducers with interleaved aluminum fingers on a piezoelectric substrate. The input transducer is implemented with fingers of equal length, while the output transducer has fingers with varied overlap. The filter operates by electrically exciting the input transducer which through the piezoelectric effect causes a surface wave along with other modes to propagate toward the output transducer. There the wave is transformed back into an electrical signal. The output transducer works in a manner similar to a digital filter and can be modeled as a tapped delay line of N fingers where 1) each finger is a delta function generator-detector of surface waves, 2) the constant propagation time between fingers is the unit delay time t , 3) the variable finger overlap (apodization) is proportional to an attenuator weight W_k and 4) the relative direction of overlap with respect to the direction of propagation determines the relative sign of that tap (see figure 1) [1].

Therefore the output is the sum of the attenuated and possibly inverted replicas of the input, each delayed by an integer multiple of the unit delay time t . The apodization function, that is the tap weights, is found by computing the fourier transform of the specified frequency response. This impulse response weighting assumes an ideal surface wave can be created which neither diffracts nor reflects [2]. Very narrow band devices may require more than 100 taps, but due to limited substrate length time sidelobe taps may be truncated by straight deletion or by applying a window to the specified frequency



KP-1021

Figure 1. Tapped delay line with unit delay time t_k and attenuator weight W_k .

response, such as Hamming the data.

The designer may adjust finger overlap and delay, therefore a wide range of transfer functions is possible. SAW devices are inherently bandpass in nature due to physical limitations. Devices lower than 10 MHz require too large of finger spacing, while devices approaching 1.5 GHz are limited by the processes used to construct the fingers.

II. THE PROBLEM

SAW filters have recently been designed specifically for low insertion loss, -60db sidelobes, small passband ripple, and/or near unity shape factor. The approach presented here stresses overall frequency response accuracy. This can be achieved by a method of correction which pre-distorts the theoretical tap weights.

Implementing a bandpass filter using the surface wave approach contains these main sources of error: 1) bulk and plate modes propagate and interfere with the surface wave, 2) the surface wave diffracts as it travels to the output transducer, 3) the fingers interact through the array due to circulating currents and regenerate other waves, 4) the surface wave reflects back off the substrate-air interface and 5) reflections off the transducer arrays create triple transit echos. The first, fourth and fifth sources can be minimized with specific fabrication techniques. The errors remaining could possibly be eliminated by a cut and tried approach, but since the taps are not fully independent a change in one tap weight affects those around it. The problem therefore lies in finding a technique to isolate consistent errors in a set of devices and applying this error to the theoretical tap weights in order to compensate for the additive errors contributed by the SAW filter approach. This technique could greatly decrease the time between passband specification and accurate filter implementation because it requires only one mask-device iteration.

III. TETAM ANALYSIS

SAW transducers are implemented in the time domain as the fourier transform of a specified frequency response. In order to correct a SAW filter, one would need to know the individual time domain contribution of each tap in its operating environment because quantitative error analysis is difficult using frequency domain data [3]. Highly accurate tap data is difficult to obtain from direct time domain measurements because the pulse exciting the SAW device must be narrow enough to resolve the higher frequency components and powerful enough to produce a useable output signal. Since the power of a constant amplitude pulse is proportional to the pulse duration, the spectral density and impulse response amplitude decrease quadratically with pulse width. Hence, the frequency range of accurate direct time domain measurements is severely limited.

A. Theory.

The impulse response of a narrow passband filter is written as [4]

$$h(t) = a(t) \cos 2\pi f_0 t + b(t) \sin 2\pi f_0 t \quad (1)$$

where $a(t)$ is the envelope of the inphase response, $b(t)$ is the envelope of the quadrature time response, and f_0 is an arbitrary frequency within the passband. The inphase response arises from the transfer function component which is symmetrical about f_0 , while the quadrature response is due to the antisymmetric component.

If two periods of $h(t)$ (figure 2a) are sampled at a $4f_0$ rate, the even numbered samples (a_{2i}) represent the inphase components, and the odd samples (a_{2i+1}) represent the quadrature components (figure 2e) [5]. The sampling process

$$h_s = \sum_{i=1}^N a_i \delta(t - \frac{i}{4f_0}) \quad (2)$$

gives rise to frequency domain images symmetric about harmonics of the sampling rate (figure 2f).

The interleaved inphase and quadrature samples (figure 2e,3a) are grouped into pairs and converted to polar form with magnitude (c_{2i}) and phase (ϕ_{2i}) given by

$$c_{2i} = \sqrt{(a_{2i})^2 + (a_{2i+1})^2} \quad (3)$$

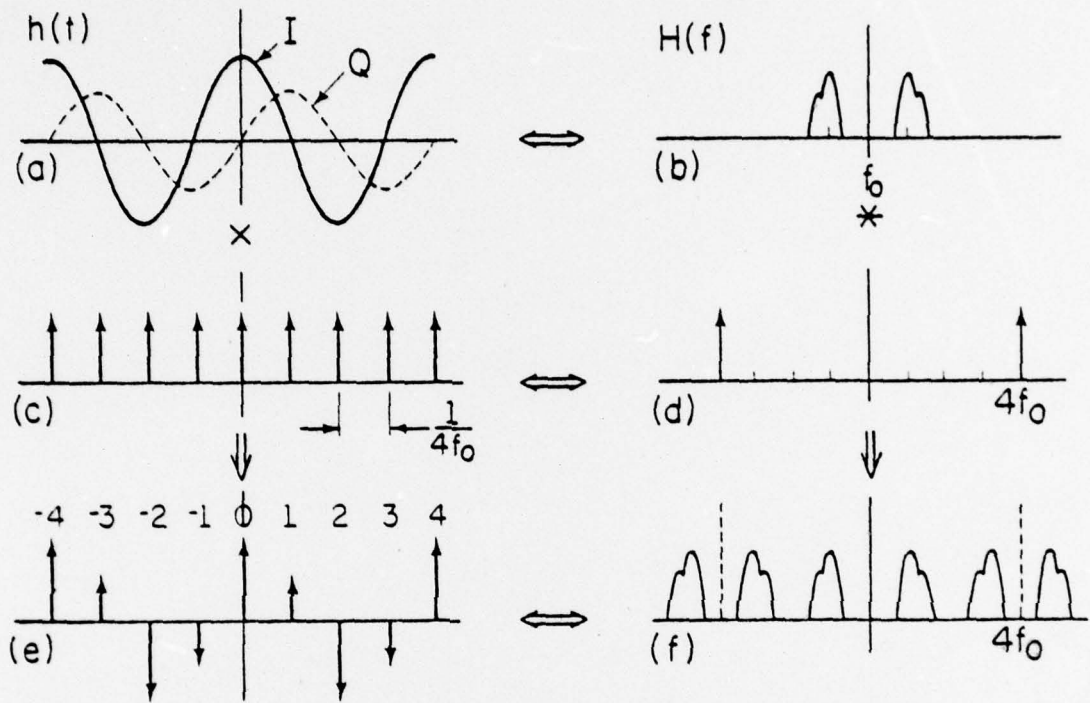
$$\phi_{2i} = \tan^{-1} \left[\frac{a_{2i+1}}{a_{2i}} \right] \quad (4)$$

The phase converts into an offset sample delay (Δt_{2i}) of $\phi_{2i}/2\pi f_0$ measured from the 2ith sampling point so that the absolute sample time is

$$t_{2i} = \frac{2i}{4f_0} + \Delta t_{2i} \quad (5)$$

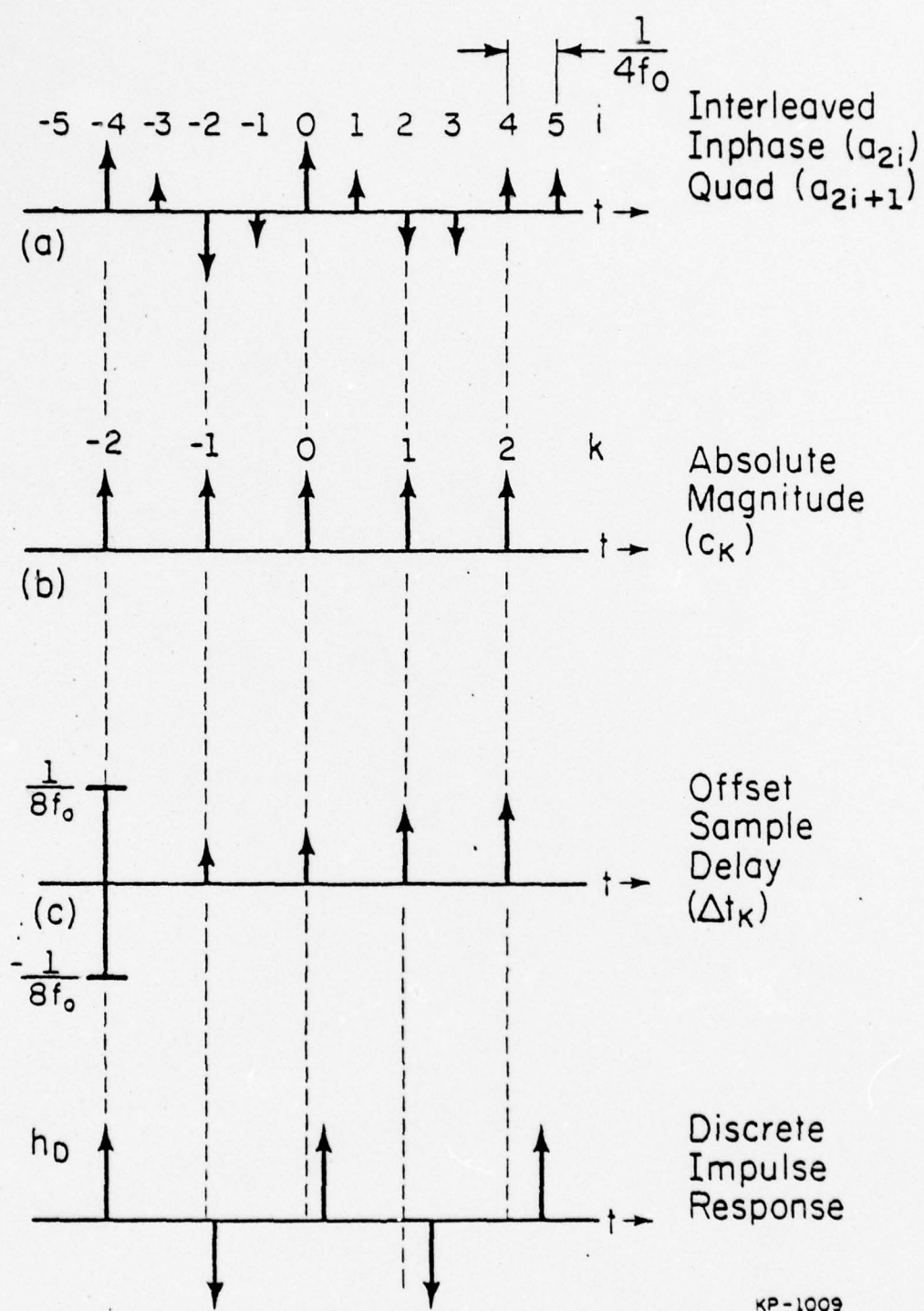
where

$$\Delta t_{2i} = \frac{1}{2\pi f_0} \tan^{-1} \left[\frac{a_{2i+1}}{a_{2i}} \right] \quad (6)$$



KP-1008

Figure 2. Time domain sampling a) two periods of $h(t)$, b) fundamental frequency response, c) sampling comb function, d) frequency comb function, e) sampled impulse response, inphase and quadrature, f) frequency domain images.



KP-1009

Figure 3. Polar conversion of samples.

is the offset sample delay and includes specified and spurious deviations from linear phase. Magnitude and offset sample delay are shown in figures 3b and 3c respectively. Incorrect choice of the sampling rate ($2f_o = F_{max}$) adds a slope to the offset sample delay which is the dual of the phase slope in the frequency domain when a time delay is present [6].

The polar conversion results in a discrete impulse response h_D nonuniformly spaced with an average interval of $1/(2f_o)$ given by

$$h_D = \sum_{k=1}^{N/2} (-1)^k c_k \delta(t - \frac{k}{2f_o} - \Delta t_k) \quad (7)$$

where $k=2i$ (see figure 3d).

B. Tap Weight and Delay Measurements

SAW transducers are modeled as tapped delay lines with each transducer element specified by a weight (W_k) and a delay (t_k) (figure 1). If individual taps have a bandwidth much greater than the filter bandwidth, the impulse response of an $N/2$ tap transducer is a series of impulses given by

$$h(t) = \sum_{k=1}^{N/2} W_k \delta(t-t_k) \quad (8)$$

which has the same form as the discrete impulse response. The polar discrete impulse response (7) is therefore useful for analysis of SAW interdigital transducers because each sample is identifiable with a transducer element. When the transfer function is measured,

transformed, and processed in accordance with the preceding discussion, the magnitude $(-1)^k c_k$ and the time $(k/2f_0 + \Delta t_k)$ represent the effective weight W_k and delay t_k of each element, respectively.

The TETAM (Transducer Effective Tap Amplitude Measurement) system enables one to accurately calculate tap weights and delays by measuring the amplitude and phase of the SAW transfer function at intervals of $2f_0/N$, where N is the number of points in the data set, typically 2048. As an example, figure 4 shows TETAM measurements of a linear phase 2 MHz bandwidth filter built on a 20 mil untapered ST quartz substrate with a designed center frequency of 100 MHz. Figures 4a and b are the measured amplitude and phase transfer functions. An N -point discrete fourier transform of these functions provides the calculated impulse response sampled at $1/4f_0$ intervals. The resulting inphase and quadrature samples (figure 4c, expanded in figure 4d) are converted to tap weights (figure 4e) and offset tap delay (figure 4f) by an algorithm based on (3) and (6). The effective tap weight and offset delay of each finger takes into account all second-order effects such as fabrication errors, diffraction, nearest neighbor interactions, fringing, bulk waves, reflections, and regeneration.

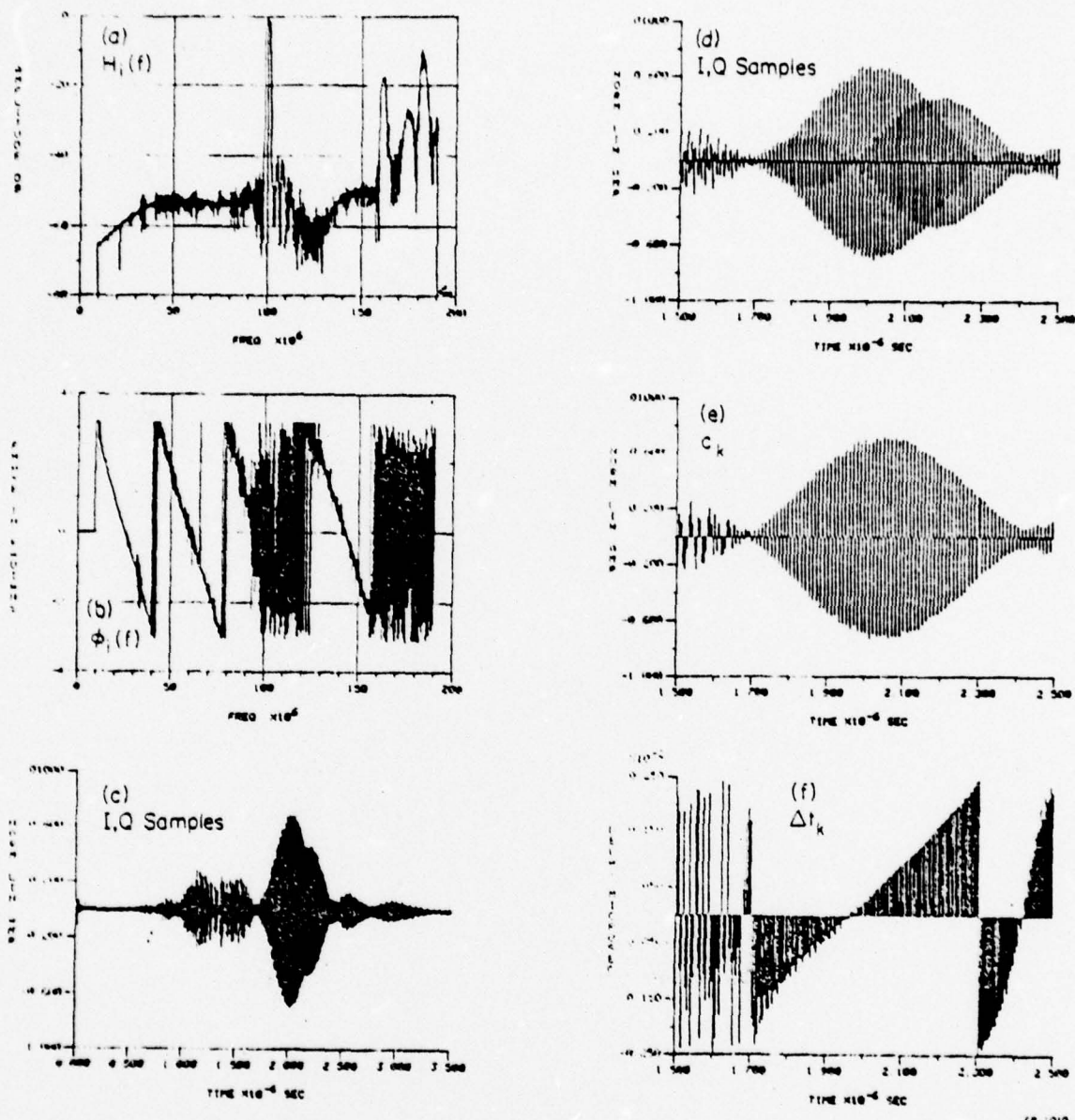


Figure 4. TETAM measured data a) frequency magnitude data, b) frequency phase data, c) Fourier transform, d) expansion of SAW impulse response, e) polar form, magnitude, f) polar form, phase.

IV. TETAM IMPLEMENTATION

The TETAM system is implemented using a digital computer to control the test process and to collect the discrete frequency domain data (see figure 5). The interface traps the TETAM control characters along with the values for the programmable attenuator and frequency synthesizer. It also contains three A/D converters which sample the vector voltmeter magnitude and phase and the RF voltmeter magnitude when commanded. The SAW device under test is buffered by two amplifiers and the system is terminated in 50 ohms. The programmable attenuator effectively replaces the vector voltmeter magnitude range switch. The vector voltmeter unlock light signal is monitored before each set of meter readings to insure that its phase lock loop is locked onto the correct frequency. A more detailed explanation is contained in the appendix.

Transducer Effective Tap Amplitude Measurement (TETAM)

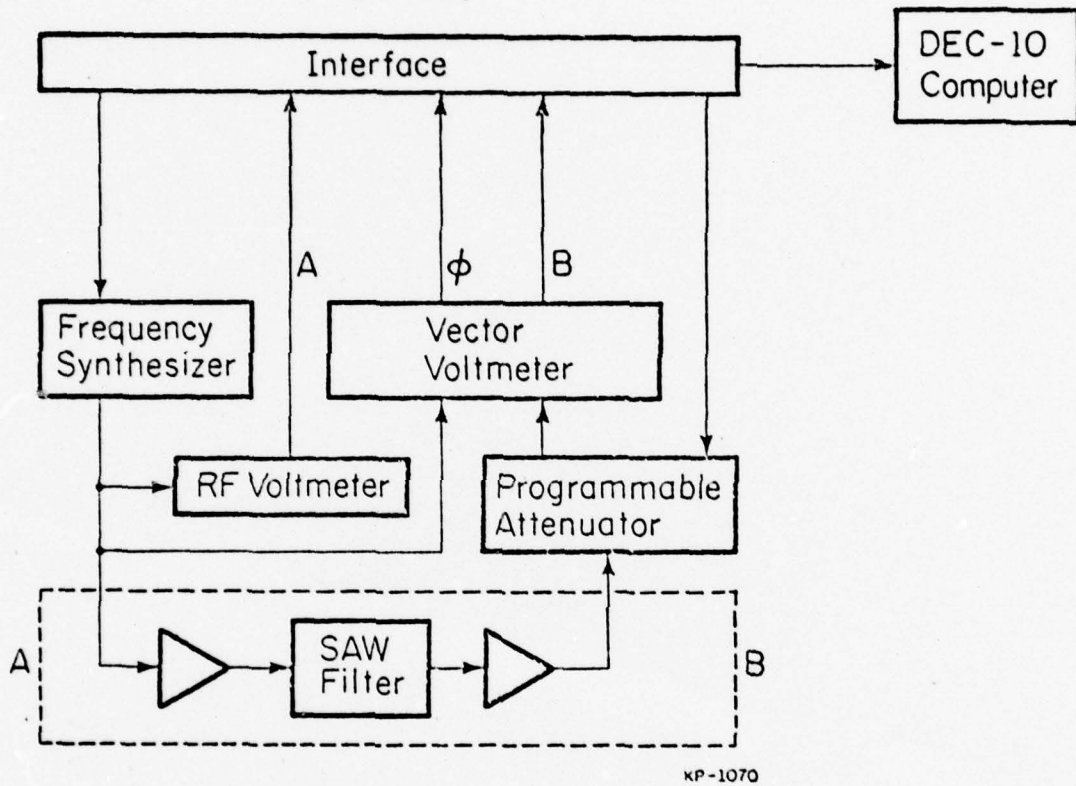


Figure 5. TETAM implementation.

V. FREQUENCY RESPONSE CORRECTION

A. Device

The TETAM data is used to redesign the device by predistorting the tap weights to compensate for errors which are consistent from device to device. The device selected for correction is an unsymmetrical passband television intermediate frequency (IF) filter implemented with inphase and quadrature samples in the form of double electrodes (see figure 6a,b). The samples of figure 6b are not similar to those of double electrodes because only the lower passband is considered. This suppresses oversampling and associates one sample with an electrode pair. The filter specifications dictate precise control of the tap weights in order to place adjacent traps at the correct frequencies. Two dual input devices (figure 7) have been fabricated next to each other on the same 128 degree Lithium Niobate substrate. The substrate back is grooved with a diamond saw at 45 degrees and absorber is placed at the ends to minimize bulk reflections. No matching networks were used and the far input transducer/output transducer combination (A->C) is used for the correction.

B. The Approach

The original IF filter configuration overall transfer function made use of the traps created by a 15 wavelength input transducer. To minimize the passband contribution of the input transducer and to evaluate errors in only the output transducer, the bandwidth of the input transducer is increased by deletion of taps (see figure 8)

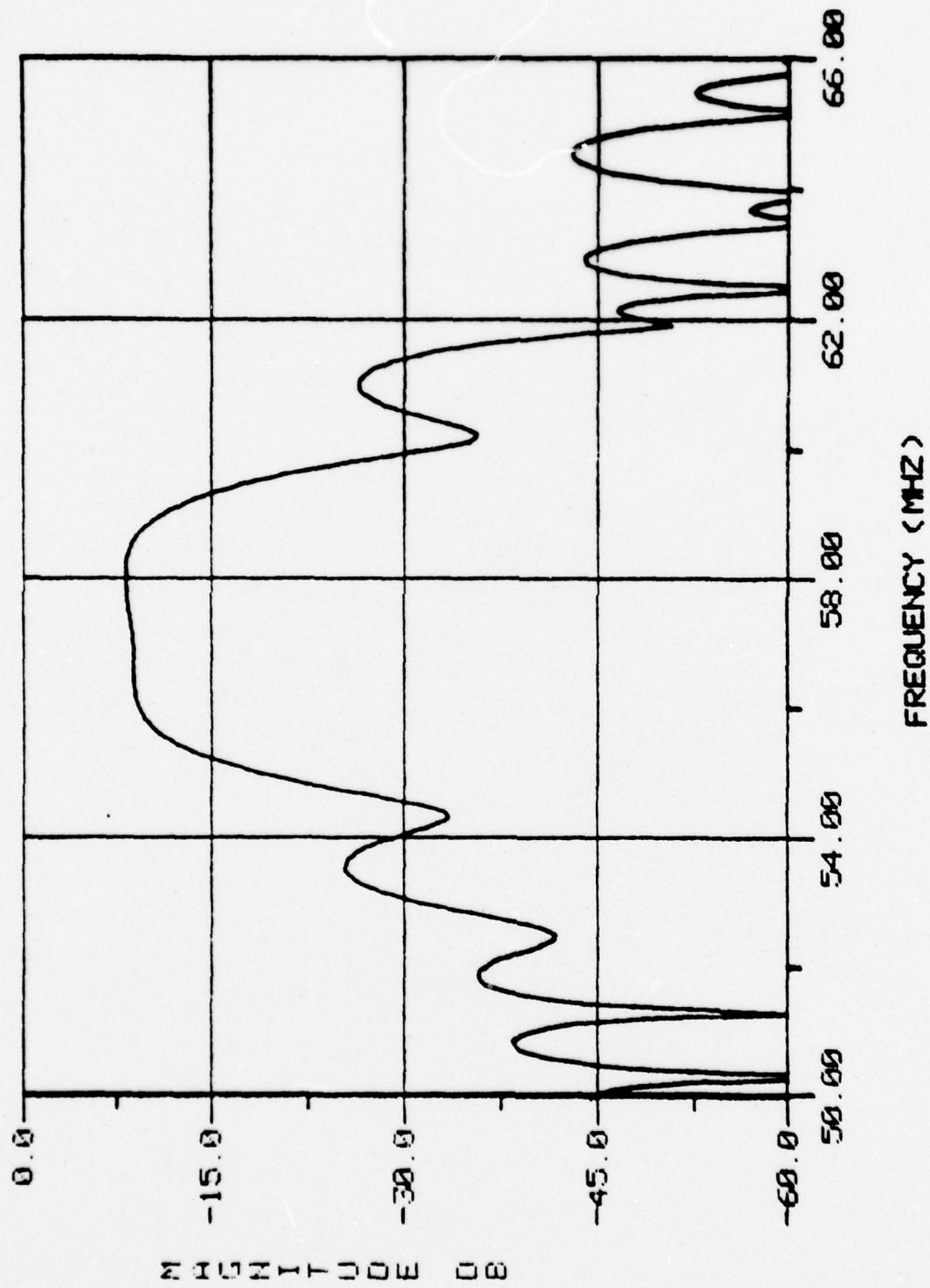


Figure 6a. Specified frequency response.

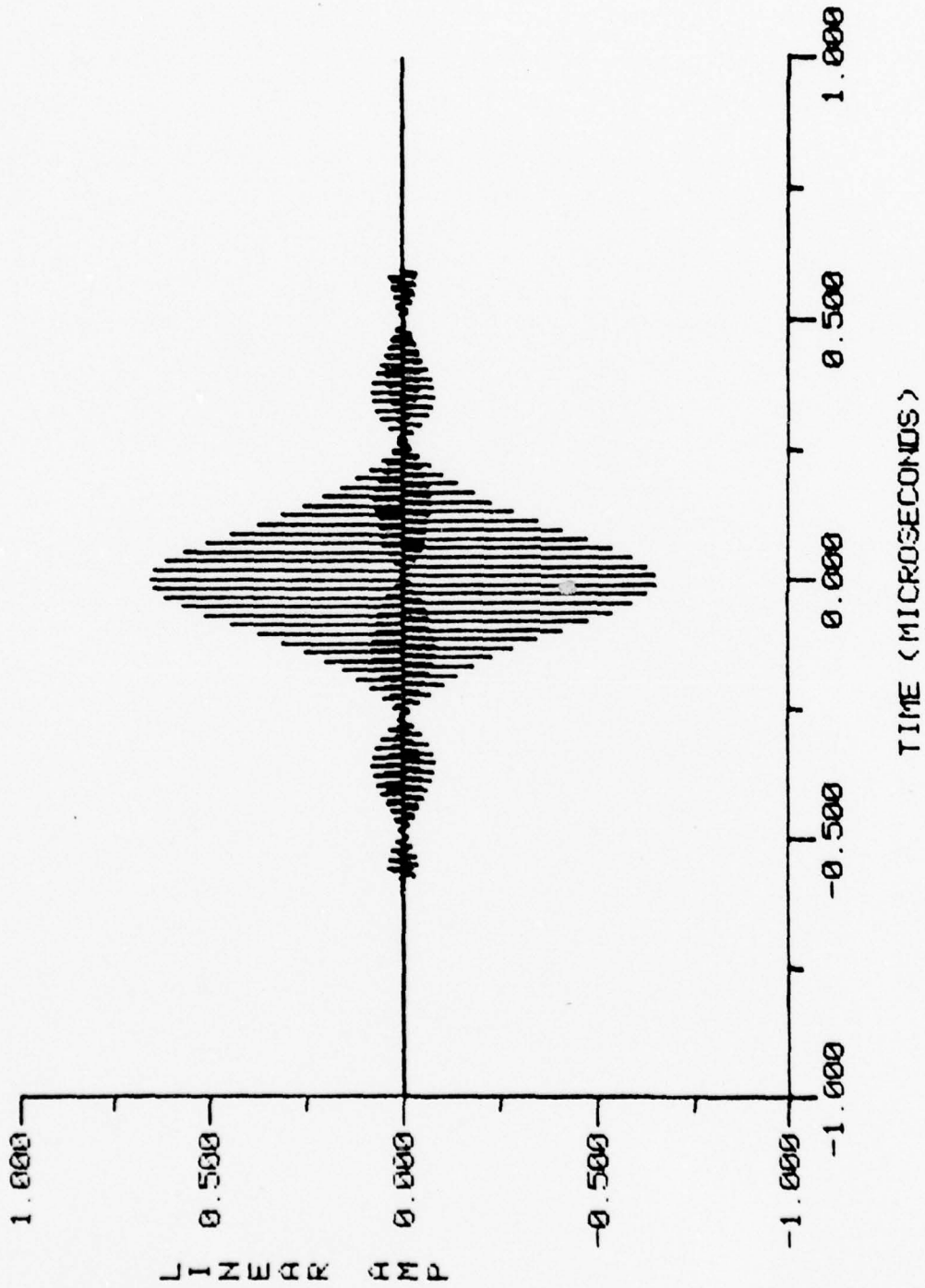


Figure 6b. Specified impulse response sampled at $F_{max} = 114$ MHz.

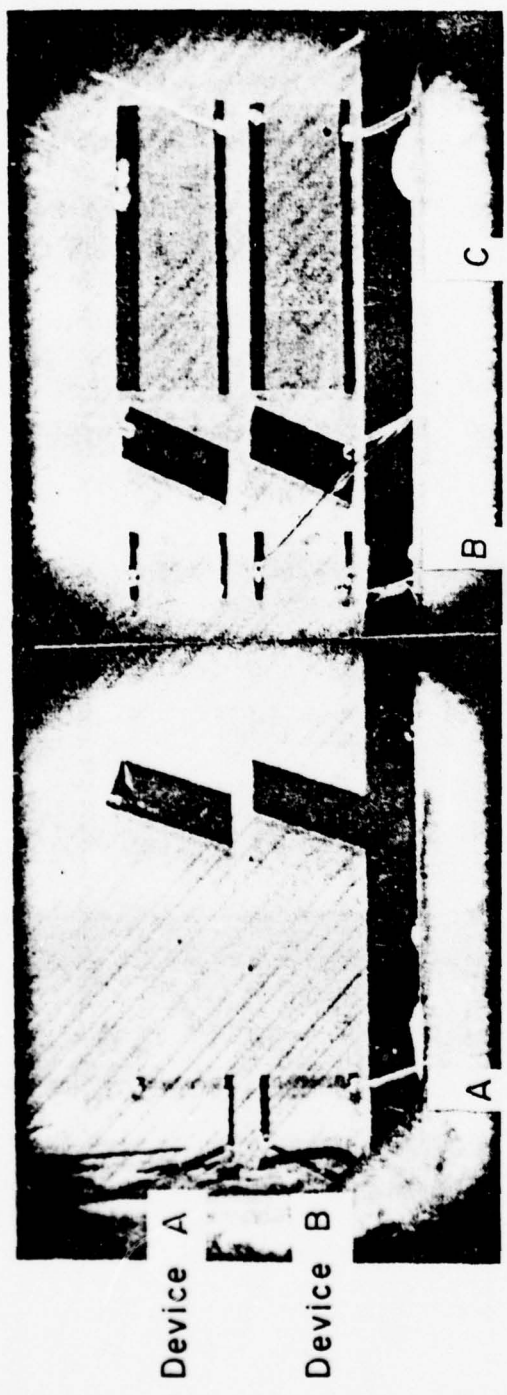


Figure 7. Actual device.

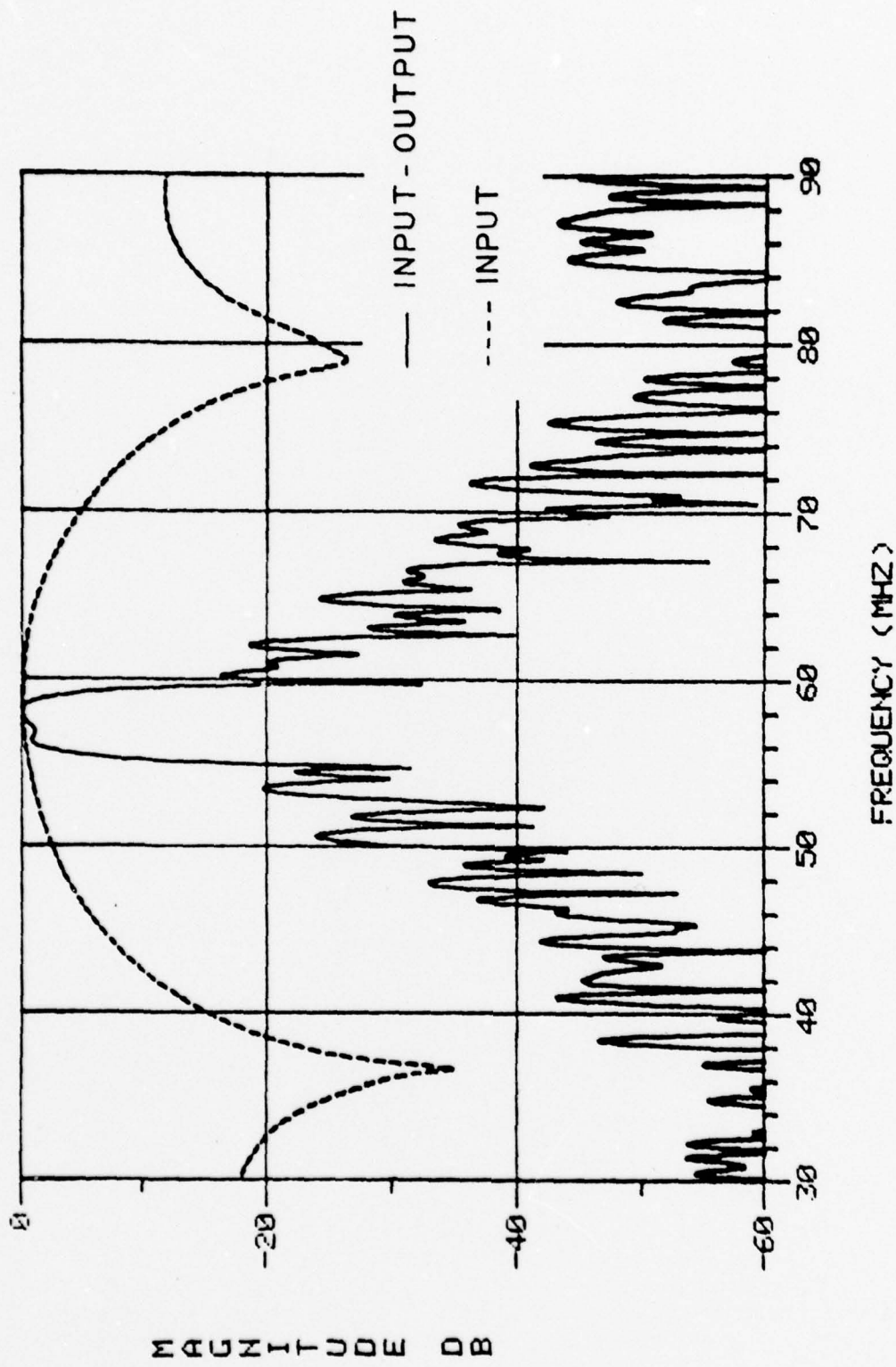


Figure 8. Experimental transfer functions.

leaving three wavelengths.

The total transfer function of a device without time delay is given by

$$H_T(\omega) = H_i(\omega) \cdot E_i(\omega) \cdot H_o(\omega) \cdot E_o(\omega) \quad (9)$$

while the transfer function between inputs is

$$H_{ii}(\omega) = [H_i(\omega) \cdot E_i(\omega)]^2 \quad (10)$$

where $E(\omega)$ is the error transfer function of that transducer.

To isolate the contribution of the output transducer the total transfer function (9) must be deconvolved with the transfer function of a single input transducer. This isolated input transducer transfer function is found by the auto-deconvolution of the input-input transfer function, giving

$$\frac{H_i(\omega) \cdot E_i(\omega) \cdot H_o(\omega) \cdot E_o(\omega)}{\sqrt{[H_i(\omega) \cdot E_i(\omega)]^2}} = H_o(\omega) \cdot E_o(\omega) \quad (11)$$

In the time domain this is equivalent to deconvolving the total impulse response by a single input impulse response. The result contains the output impulse response, its errors, and errors due to the propagation of the surface acoustic wave.

C. TETAM Data Measurement

The TETAM program input parameters are set to measure frequency domain data from zero to twice the specified center frequency of the device. This results in

$$\Delta t = 1/2F_{\max} = 1/4f_o \quad (12)$$

giving one sample per double electrode. In the process of deconvolution the experimental transfer function sampling rate is carefully adjusted so the two similar passbands fall on top of each other. Without this consideration the deconvolution in the transition bands could reach large values when a large number is divided by a small one. The center frequency cannot be determined by the largest frequency domain value because this is not a symmetrical passband. Therefore two points in the symmetrical section of the passband (-6db) are selected, their frequencies summed and compared with the theoretical -6db points by

$$\begin{aligned} \frac{F_{\max}}{\text{THEO}_{-6\text{db}}} (\text{EXP}_{-6\text{db}}) &= \frac{114}{55.325 + 59.313} (56.760 + 60.635) \\ &= 116.742 = \text{Correct } F_{\max} \end{aligned} \quad (13)$$

TETAM is run over zero to this more exact F_{\max} for both the input-input (A->B) and input-output (A->C) transfer functions. It is important to use a large number of frequency samples (ie. small Δf) to give a sufficiently large time range (total time range = $1/\Delta f$). This insures that reflections off the crystal edges, triple transit echo or other long time duration components are not aliased back into the time region of interest.

D. Experimental Input Response

The input-input frequency data is transformed to the time domain and time truncated over greater than twice the theoretical time duration to isolate the contribution of the surface wave. When truncating before deconvolution a sufficient time range must be

retained in order to reconstruct an accurate representation, because in the process of convolving two functions the resultant time range is the sum of the original time ranges (see figure 9a).

The truncated input-input time data is transformed to the frequency domain and time shifted to exactly $t=0$ (see appendix, Aphaz) because the deconvolution is most easily performed about time zero (figure 9c). To implement the auto-deconvolution process the square root of the frequency domain magnitude is taken while the phase is divided in half. In the case of the deconvolution to a $\text{sinc}(x)$ function the phase is mostly zero and one must offset the experimental phase by π radians in alternating sidelobes (figure 9d). This is accomplished by creating a theoretical $\text{sinc}(x)$ function and using its phase to modulate the experimental (figure 9e). After time truncation to exactly the theoretical time duration the experimental SAW transfer function of a single input transducer at $t=0$ results.

E. Output Experimental Response

The input-output frequency data is also time truncated over the sum of the output and the input time durations and time shifted to $t=0$. After deconvolution the data is time truncated again to the theoretical $\pm .6 \mu\text{sec}$ duration, because only this range contains taps which may be altered. Figure 10 is the surface acoustic wave contribution of the isolated output transducer in its own environment, that is the experimentally derived tap weights.

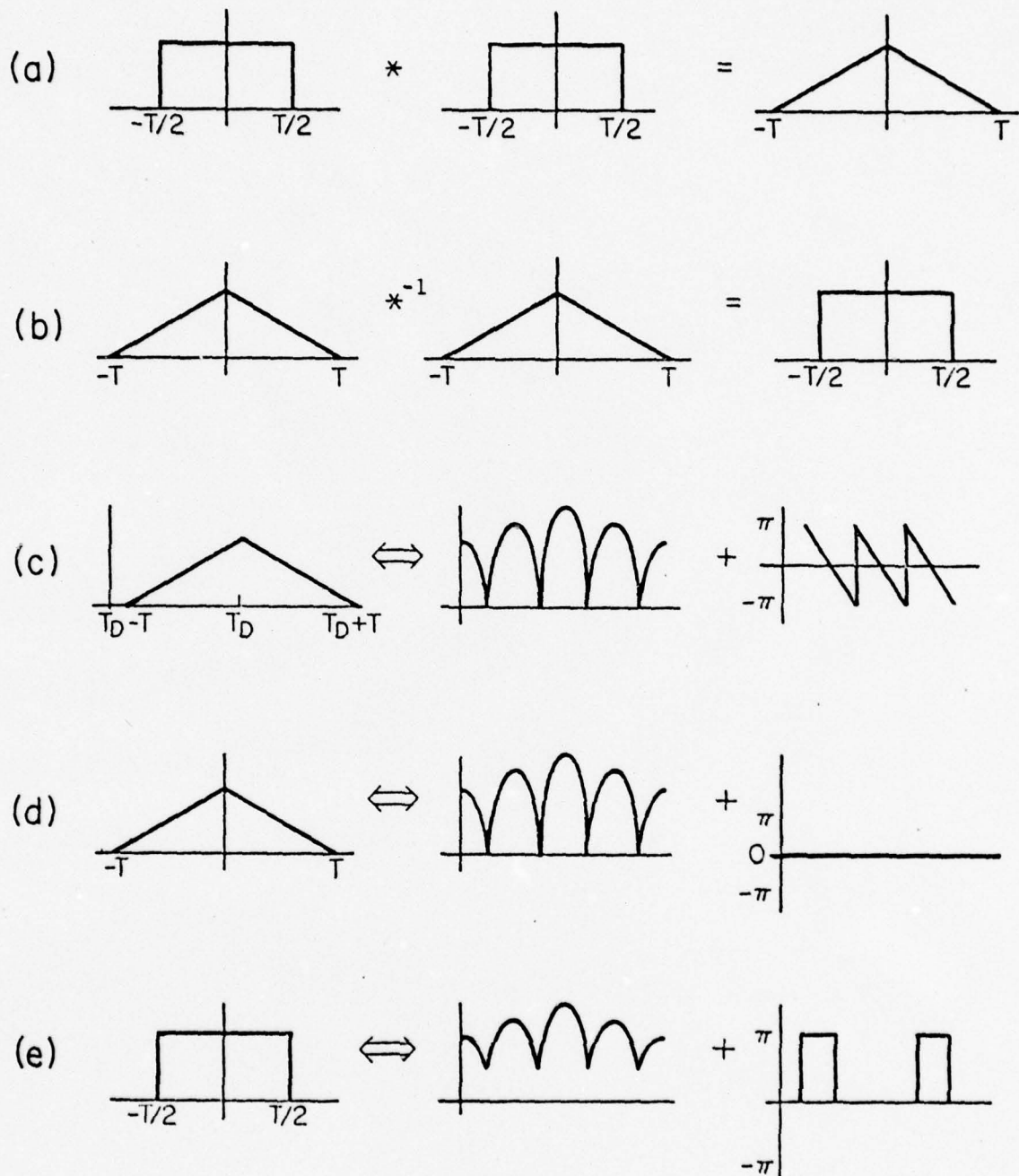


Figure 9. Auto deconvolution a) convolution, b) auto-deconvolution, c) transform pair with time delay, d) transform pair at $t=0$, e) auto-deconvolution, square root of magnitude, phase offsets.

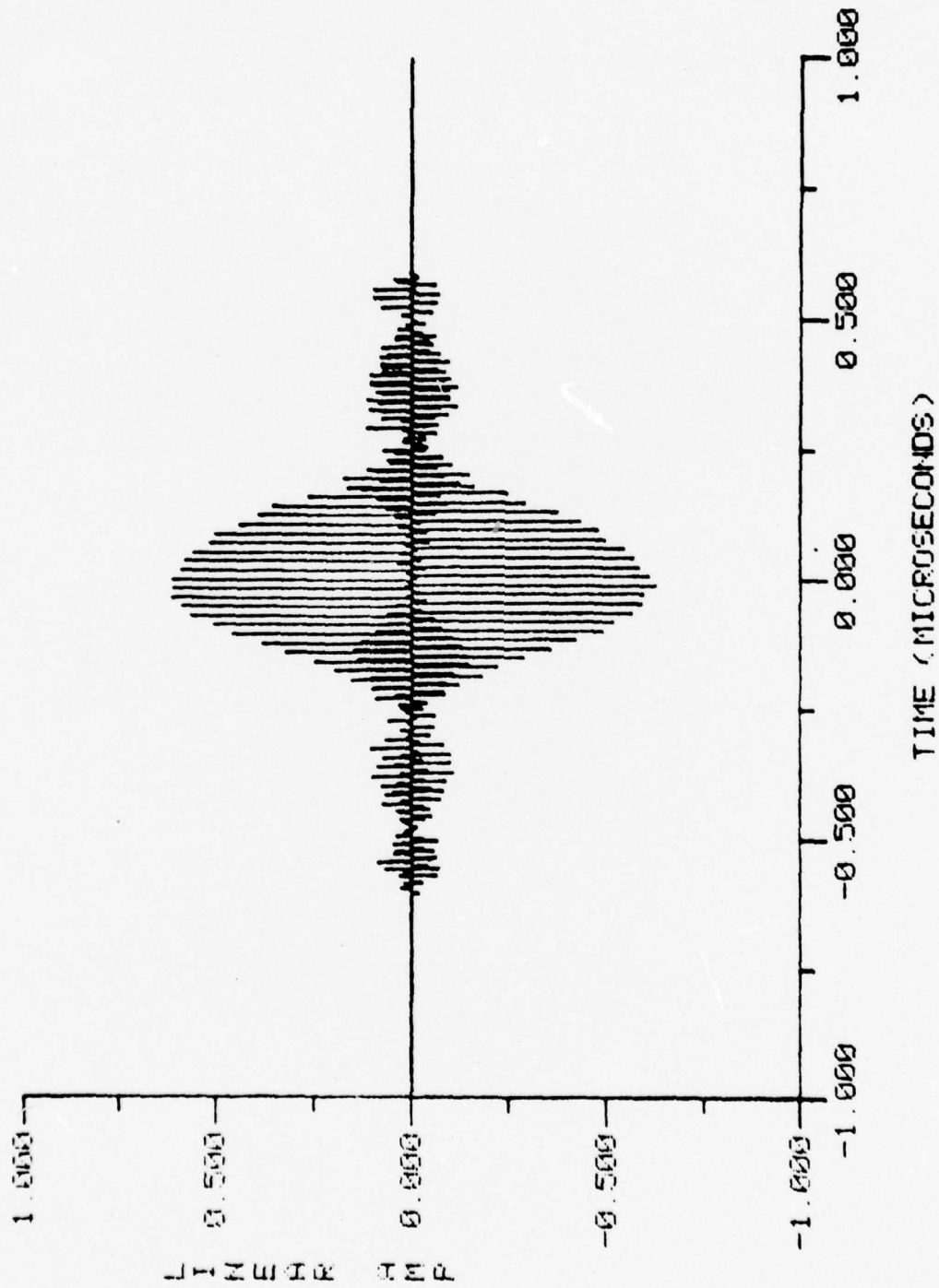


Figure 10. Experimentally derived tap weights.

F. Comparison with Theoretical

Figure 11 is a comparison of the experimental surface wave output transducer frequency responses to the specified response. Note the large errors in the positioning of the adjacent traps. To isolate these errors the two sets of experimental tap weights are individually compared with the theoretical tap weights in the time domain on a tap by tap basis. Two errors that are not addressed in this study are insertion loss and frequency scaling. The experimental insertion loss is not zero, therefore in order to have an accurate comparison (ie. minimum error) the experimental weights must be scaled.

$$\text{ERROR}(t) = \text{THEO}(t) - \text{BETA} * \text{EXP}(t) \quad (14)$$

The scaling factor (BETA) is calculated to minimize the contribution of the theoretical weights in the error file and is quickly found using Newton's method [7]. See appendix, Minerr.

The experimental device responses are not centered at the specified frequency. This frequency scaling error is best handled by accurate photo-reduction procedures. An investigation into the accuracy of using the previously mentioned -6db frequency points has been undertaken. To implement this procedure the frequency scaling portion of the MINERR program is activated and a double convergence (frequency and magnitude scaling) procedure takes place. See appendix. The results have shown that the assumption of the -6db points being entirely in the symmetrical portion of the passband is quite accurate. The results of the MINERR analysis are shown in figure 12a,b and figure 13a,b for each device.

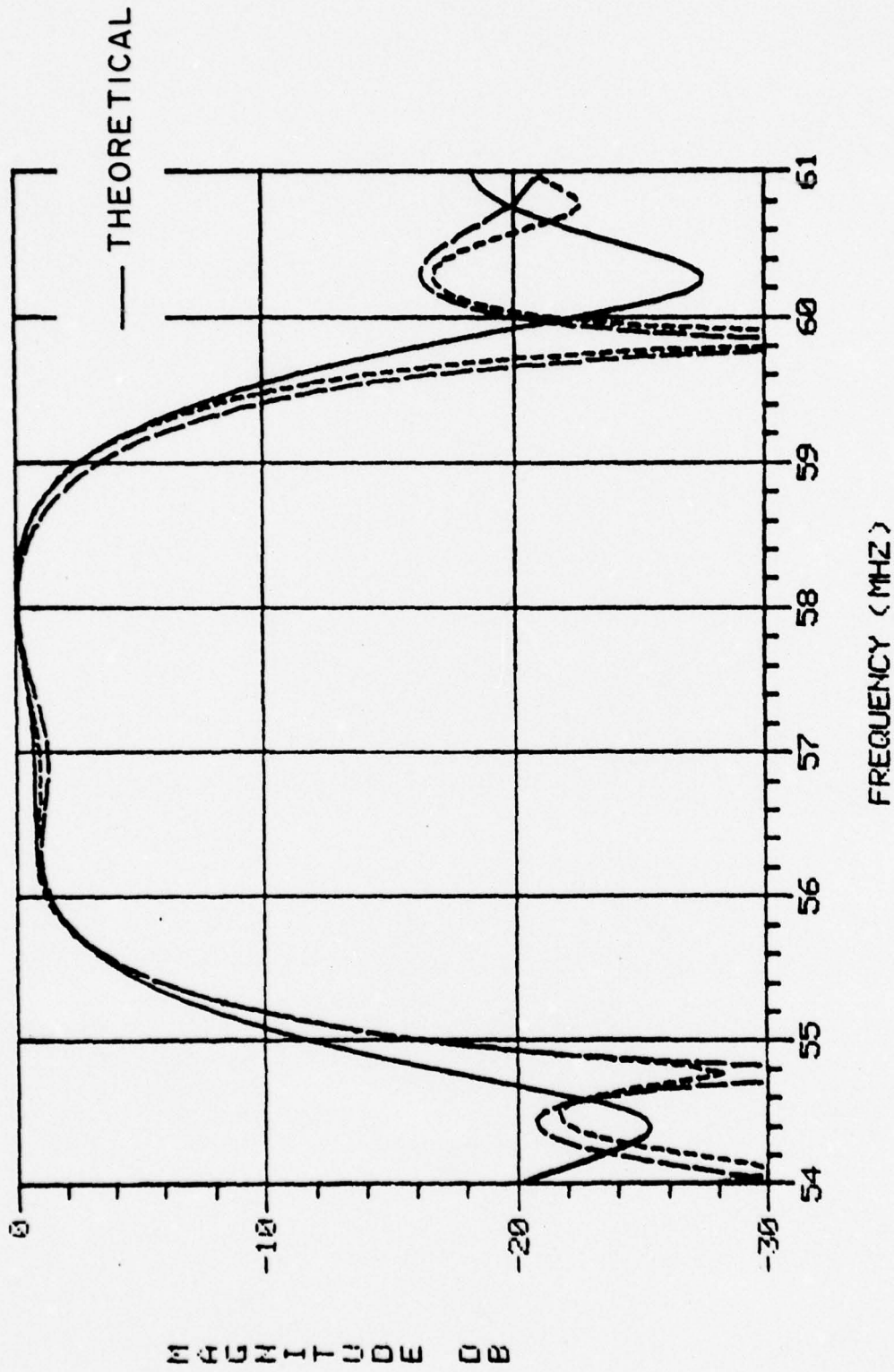


Figure 11. Comparison of the theoretical and the two SAW experimental frequency responses.

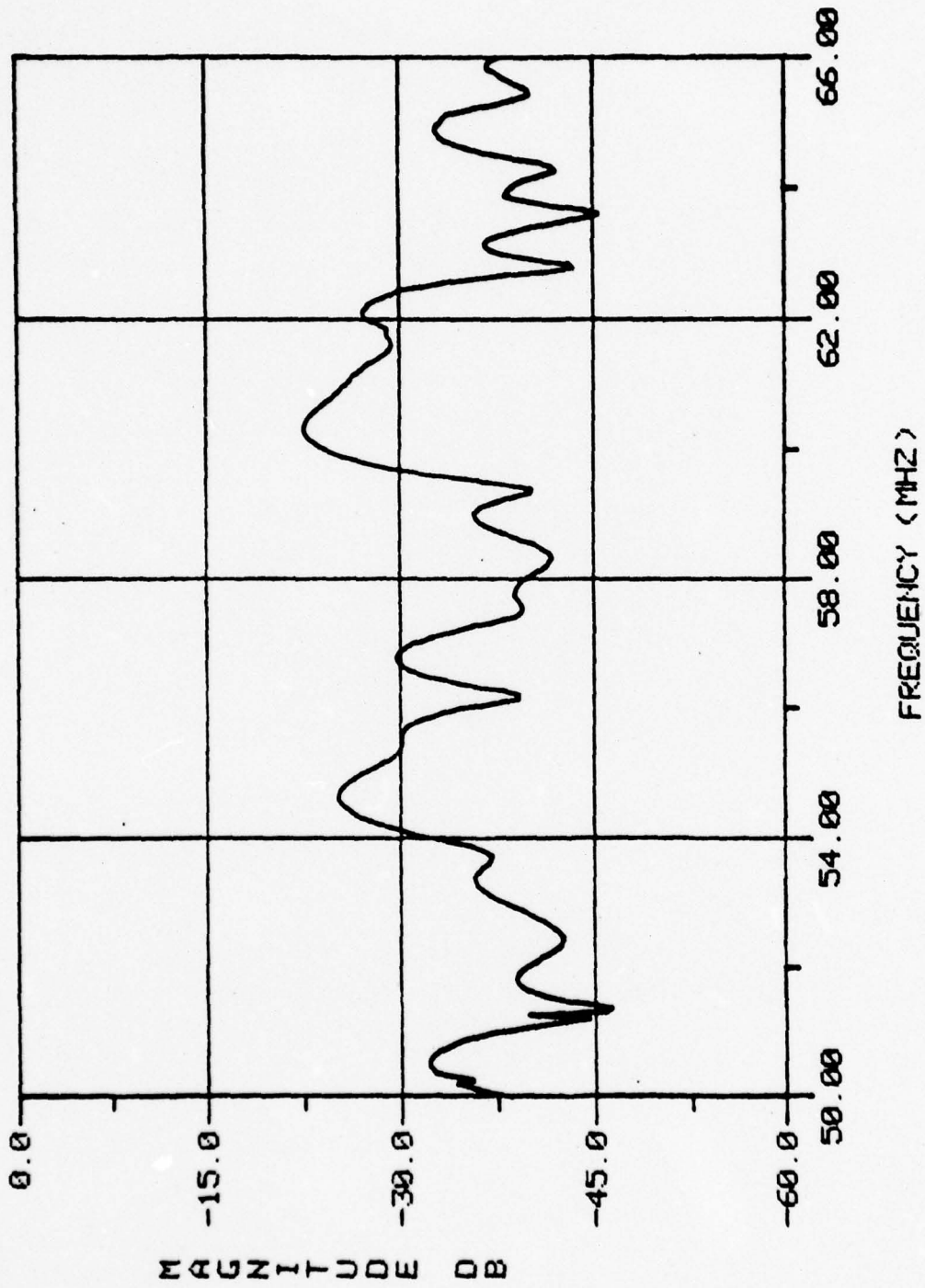


Figure 12a. Error in device A, frequency response.

10/1/61

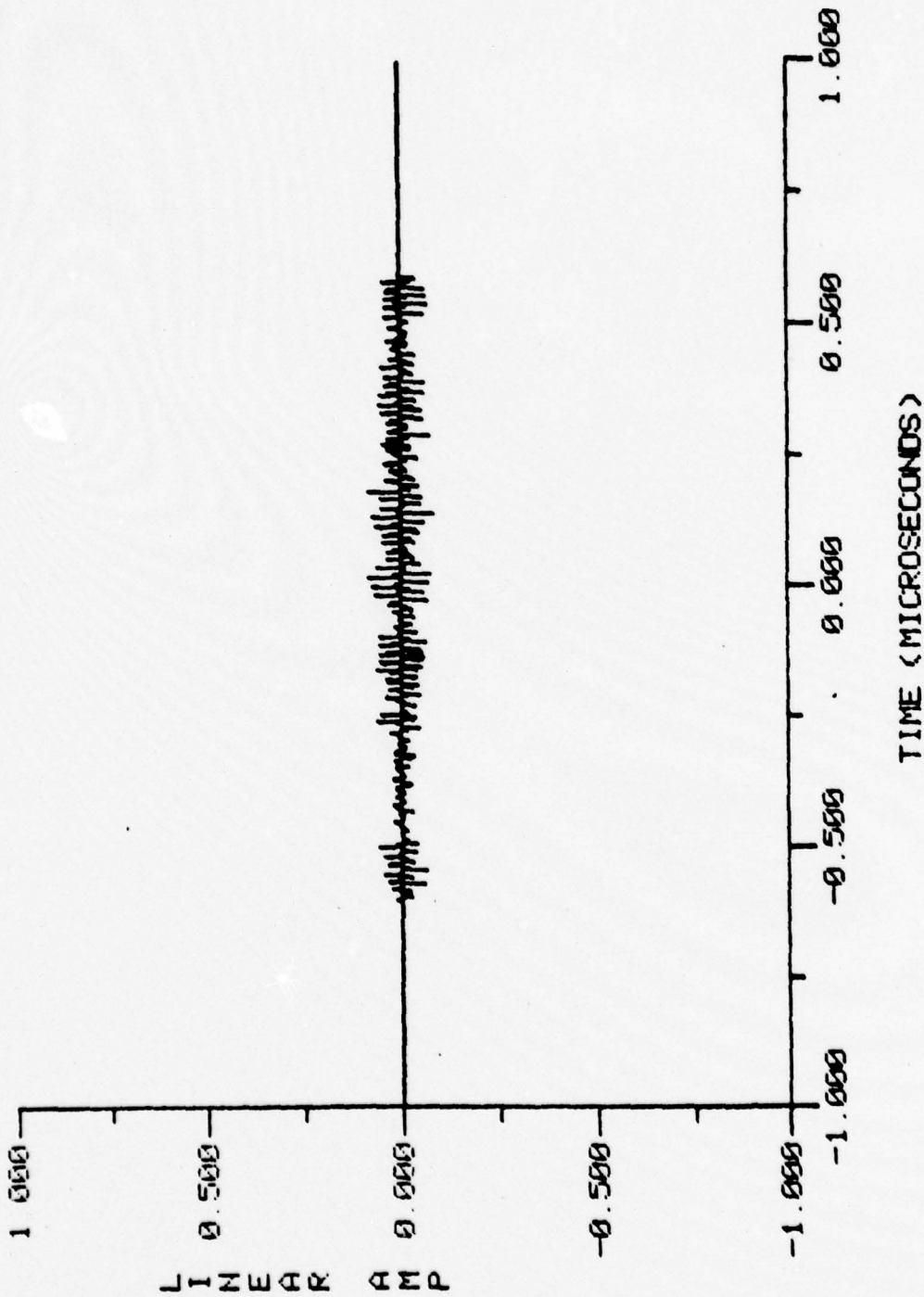


Figure 12b. Error in device A, impulse response.

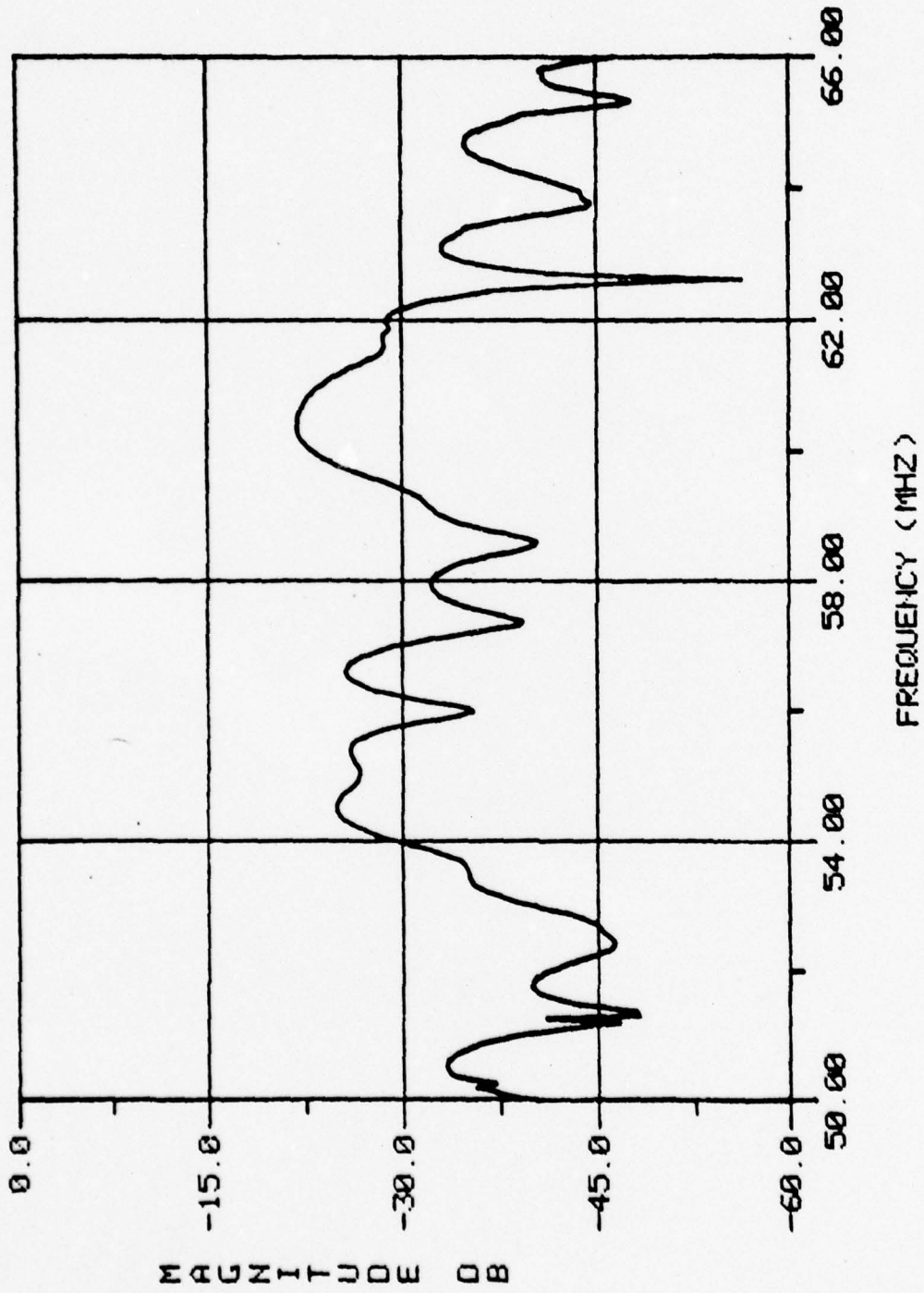


Figure 13a. Error in device B, frequency response.

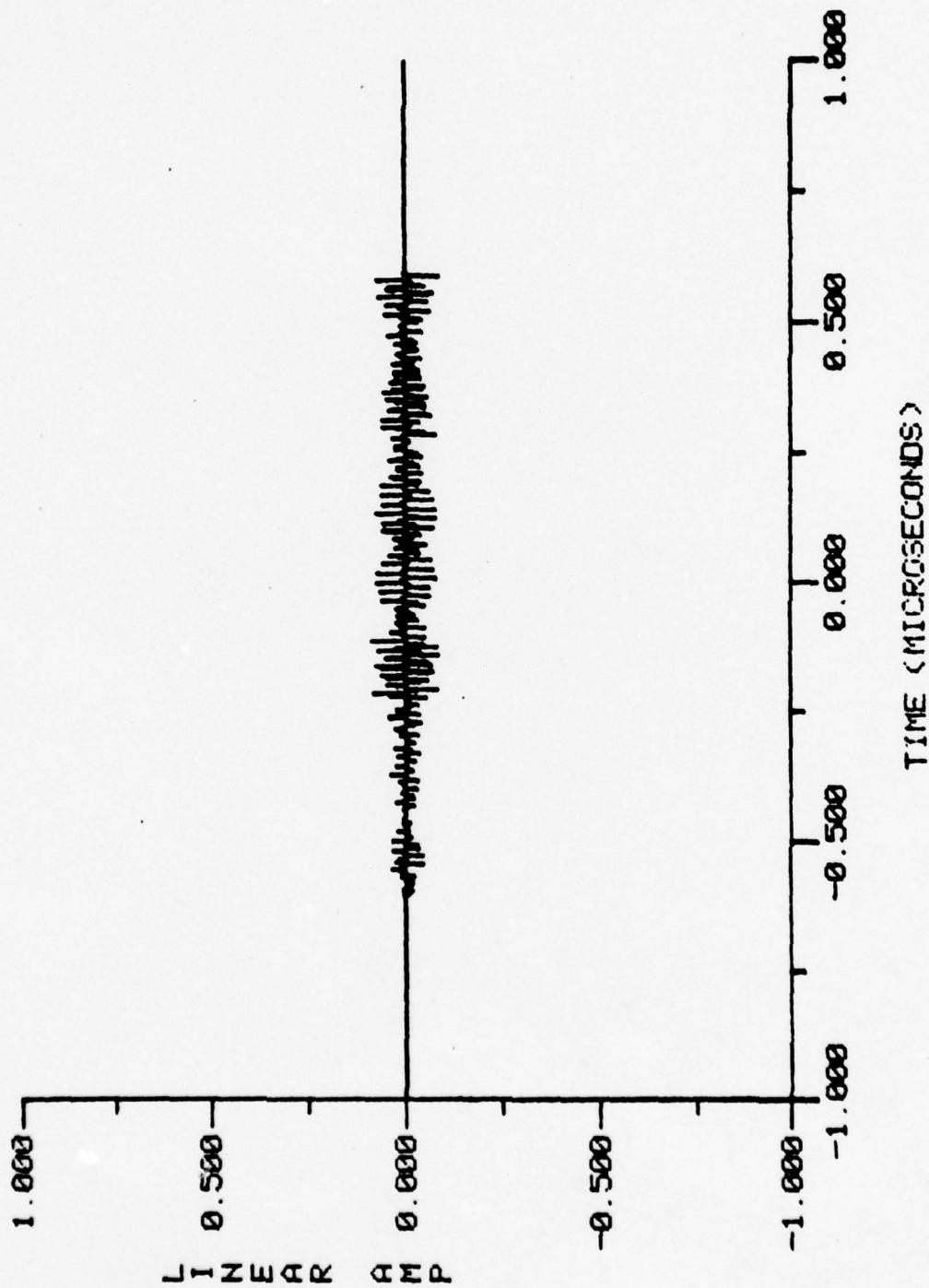


Figure 13b. Error in device B, impulse response.

This study is concerned with the isolation of a consistent error, therefore the two time error files are averaged (figure 14a,b) to give their common error with respect to the theoretical. The difference between the devices (figure 15) is a measure of inconsistency from device to device and as such is unique to a specific device. That is, an attempt to correct a response below this level would favor either device, but not both. The analysis of a larger number of devices would lower the inconsistency and produce a more accurate average error file.

G. Consistent Error Equalized Response

Equation 14 defines the method of adjusting or predistorting the theoretical tap weights. The new tap weights become the sum of the error and the original theoretical files because only then can the scaled experimental file be equal to the original theoretical tap weights. Figure 16a is a plot of the new frequency response superimposed on the original theoretical frequency response. Note the adjacent trap positions have moved out from the center of the passband to correct for the original consistent error. This frequency expansion is reflected in the time domain compression of figure 16b. This marked compression suggests that the nearest neighbor effect has increased the weight of these taps in the original device.

If two new devices are fabricated with the exact same steps and variables as the original, but using the new tap weights, the results are expected to closely resemble those of figure 17a,b and figure 18a,b. The new experimental frequency responses are very close to

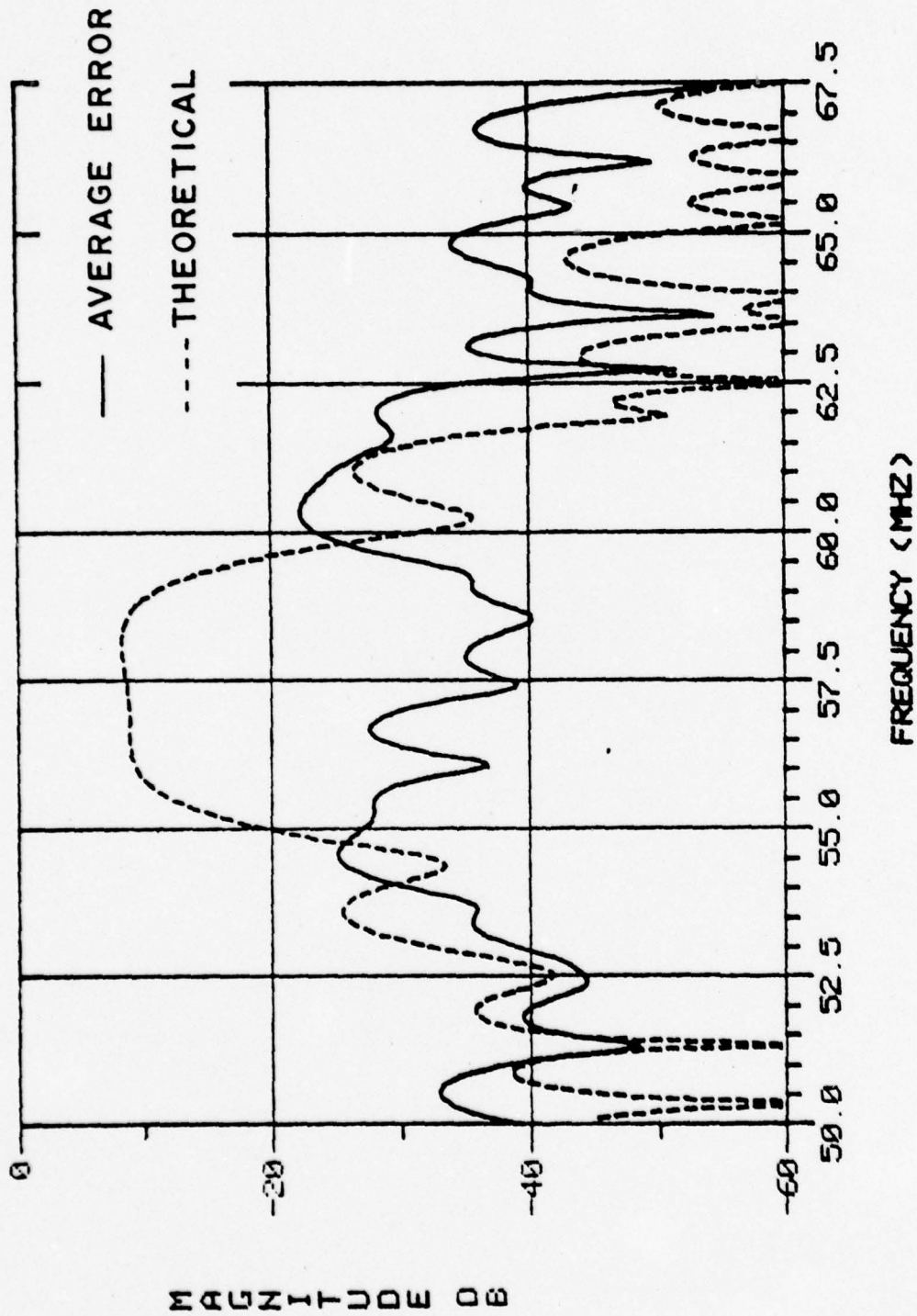


Figure 14a. Average error frequency response.

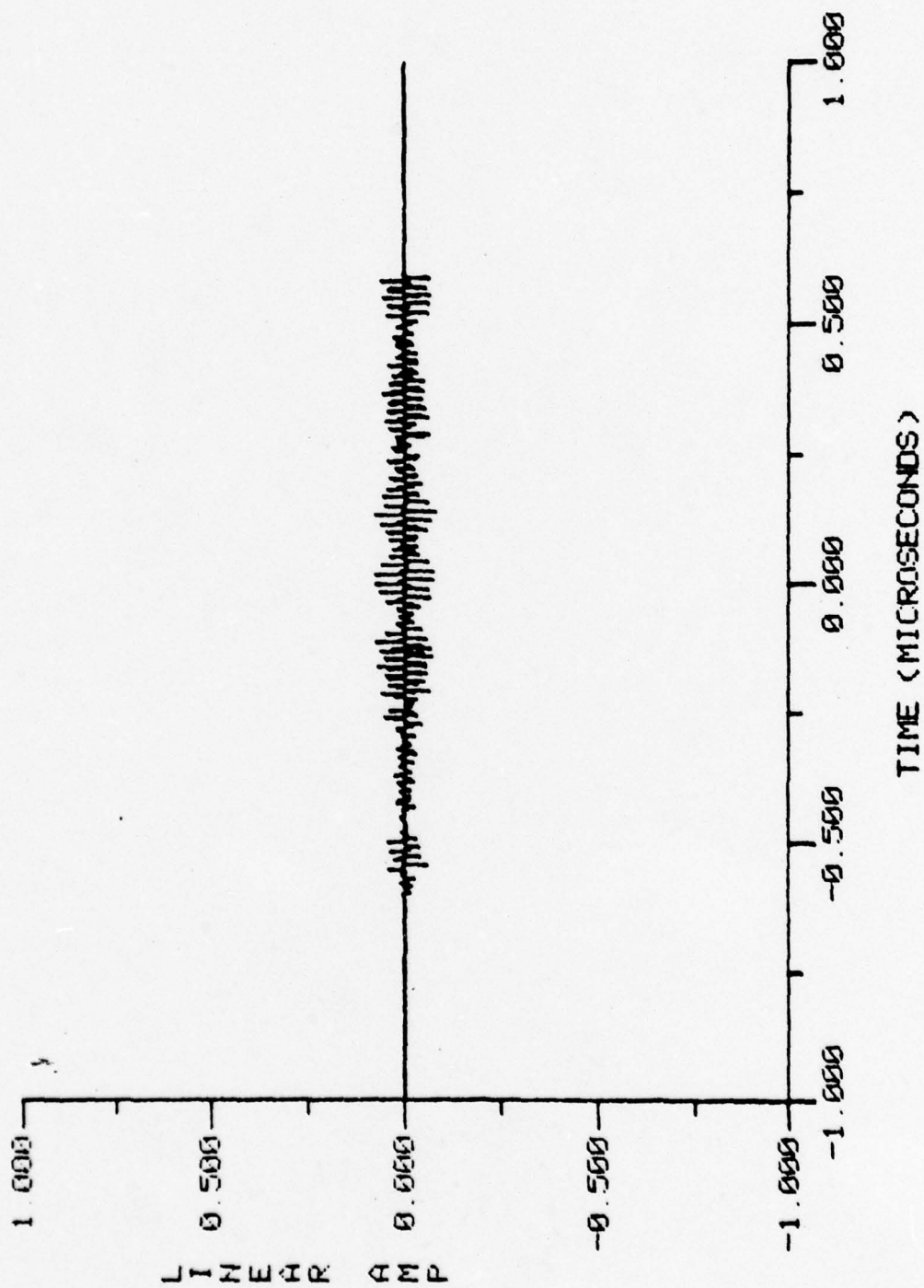


Figure 14b. Average error impulse response.

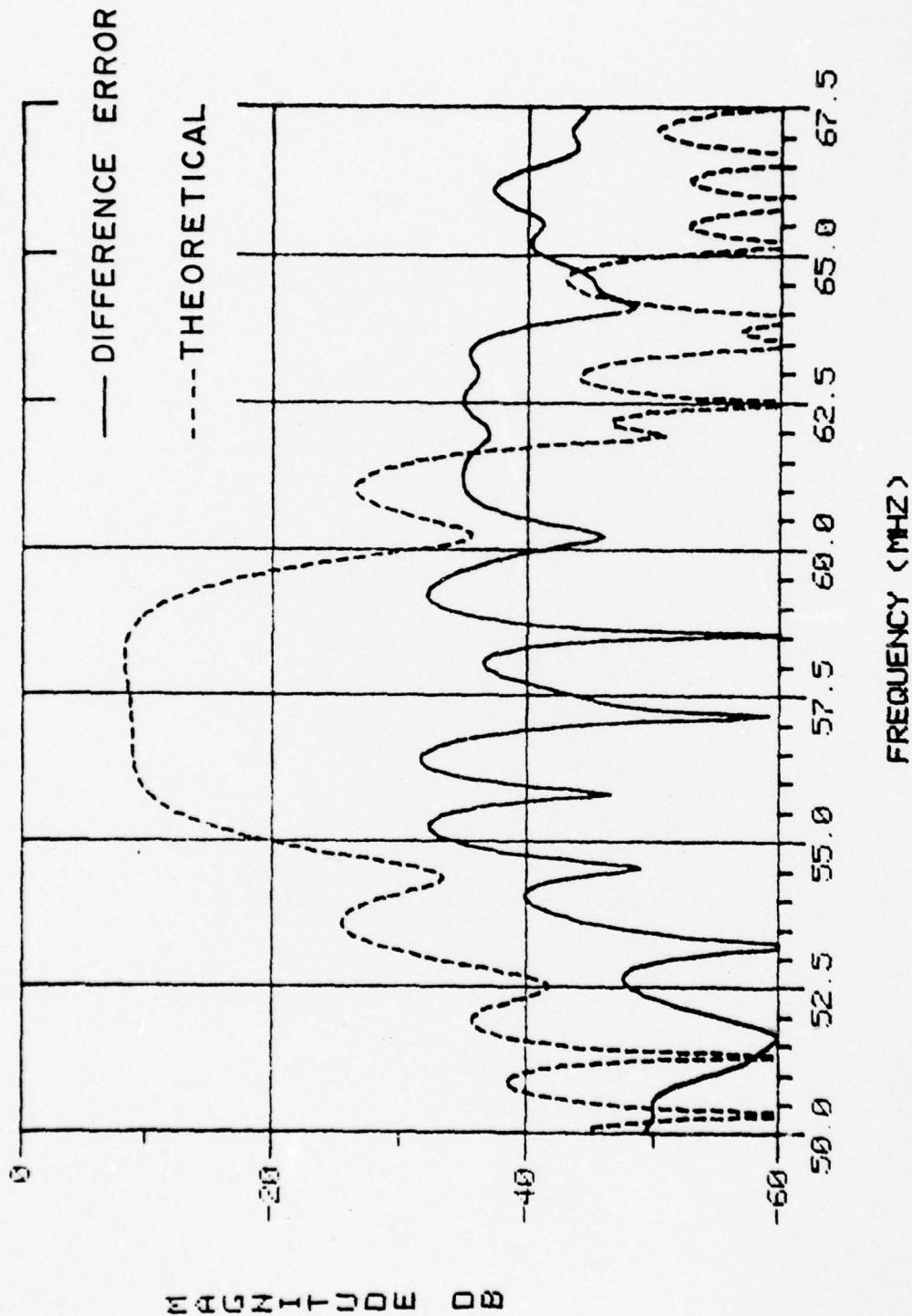


Figure 15. Difference error

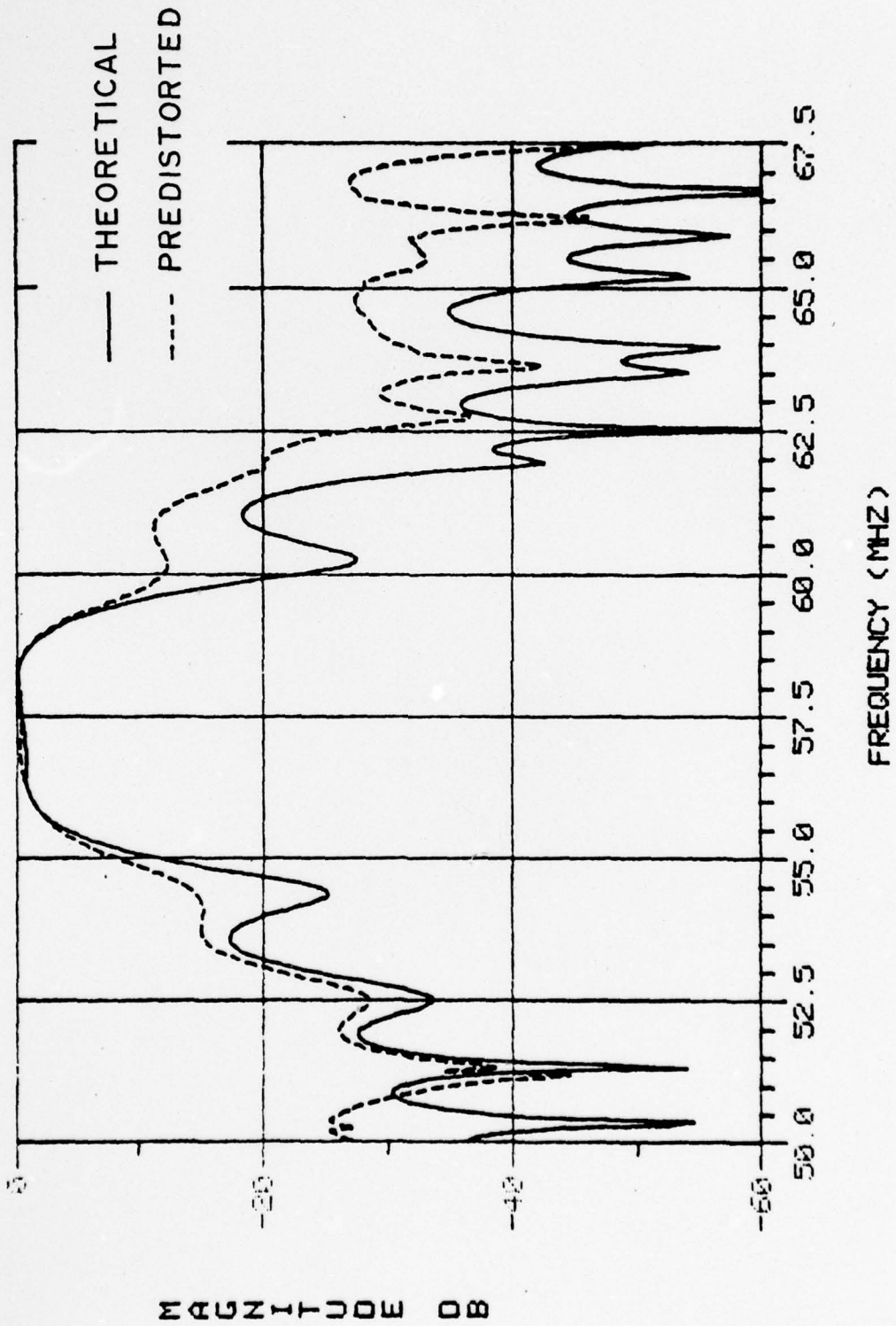


Figure 16a. Predistorted file frequency response.

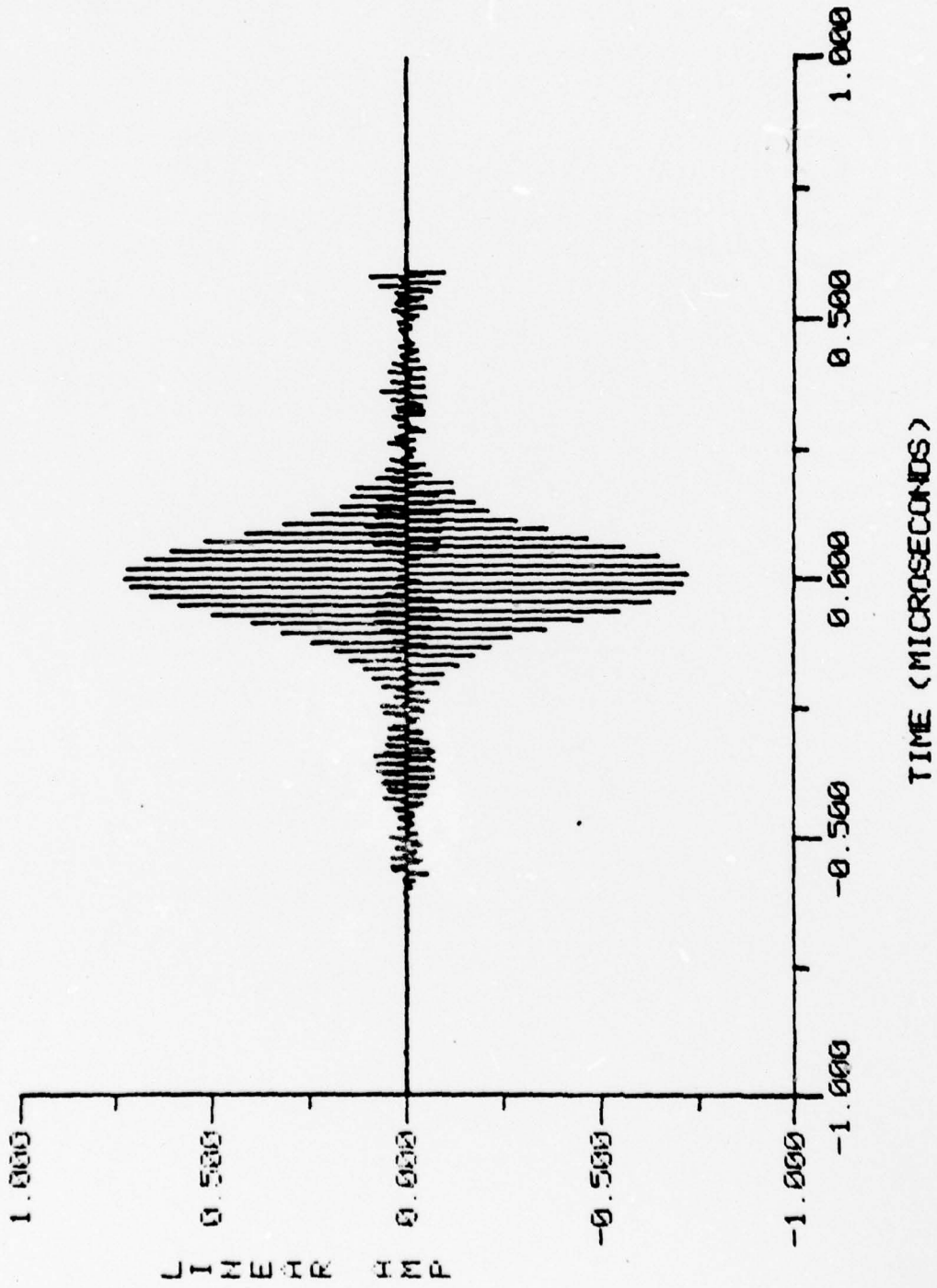


Figure 16b. Predistorted file, new tap weights.

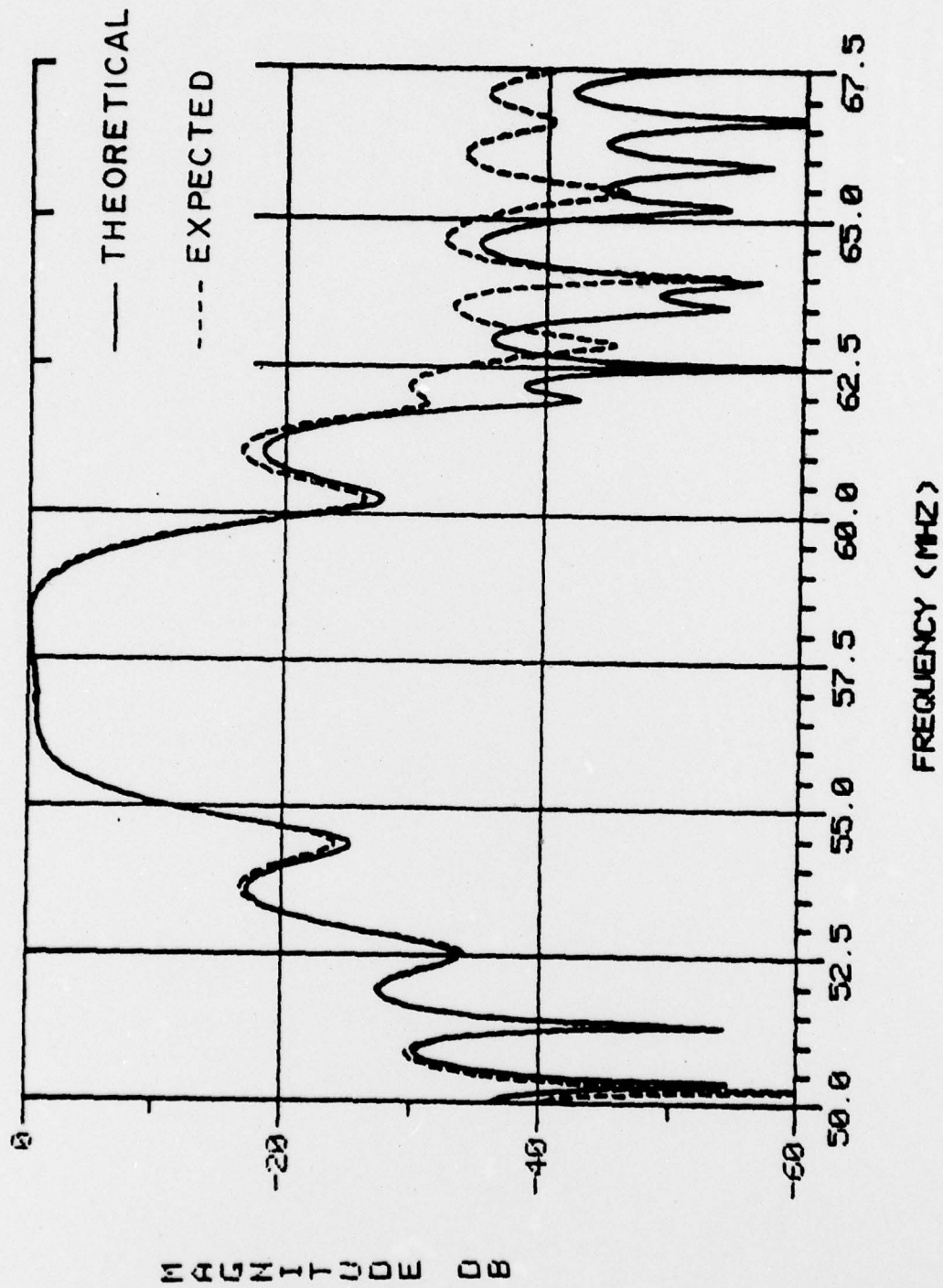


Figure 17a. Expected results device A, frequency response.

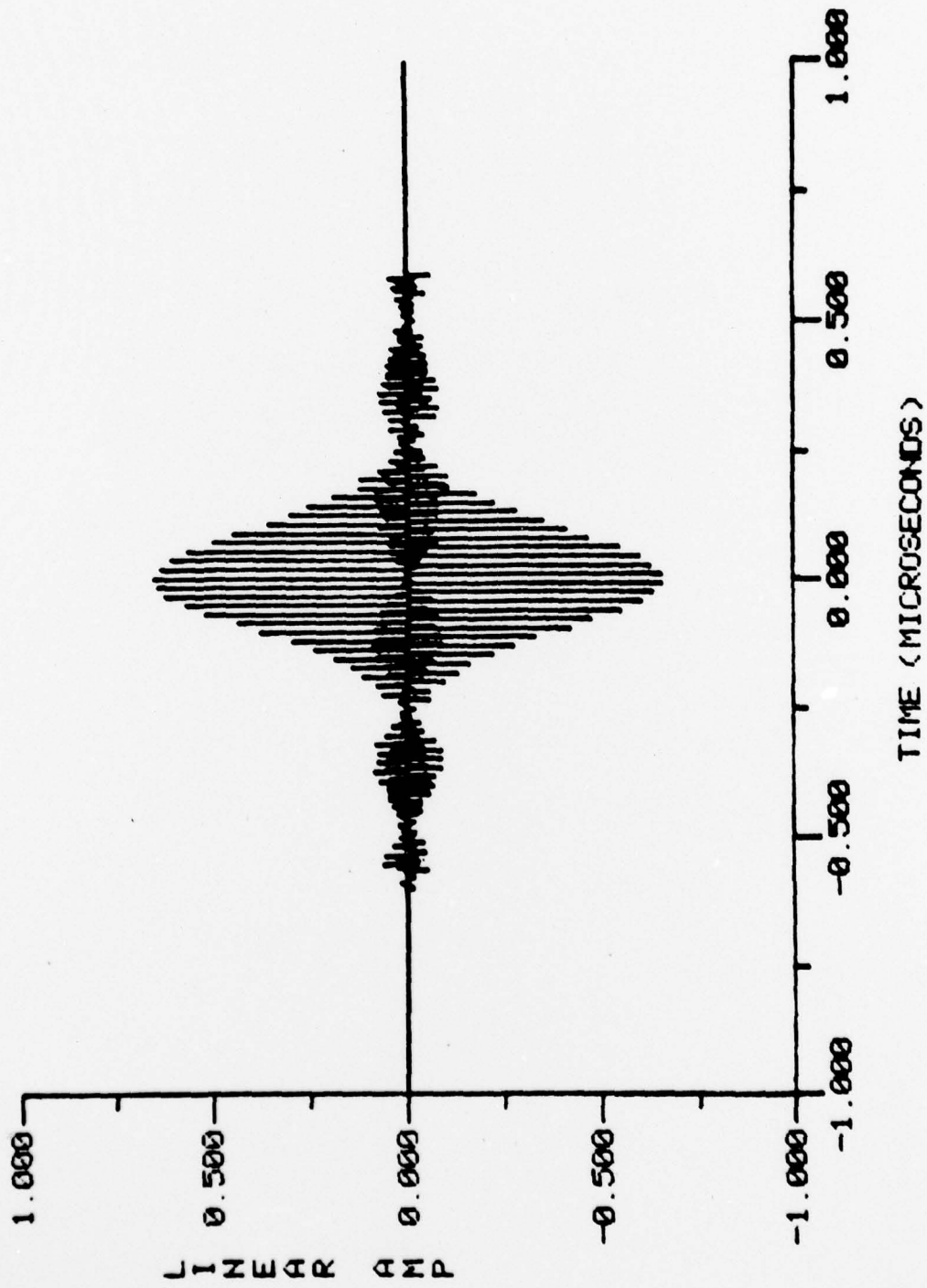


Figure 17b. Expected results device A, impulse response.

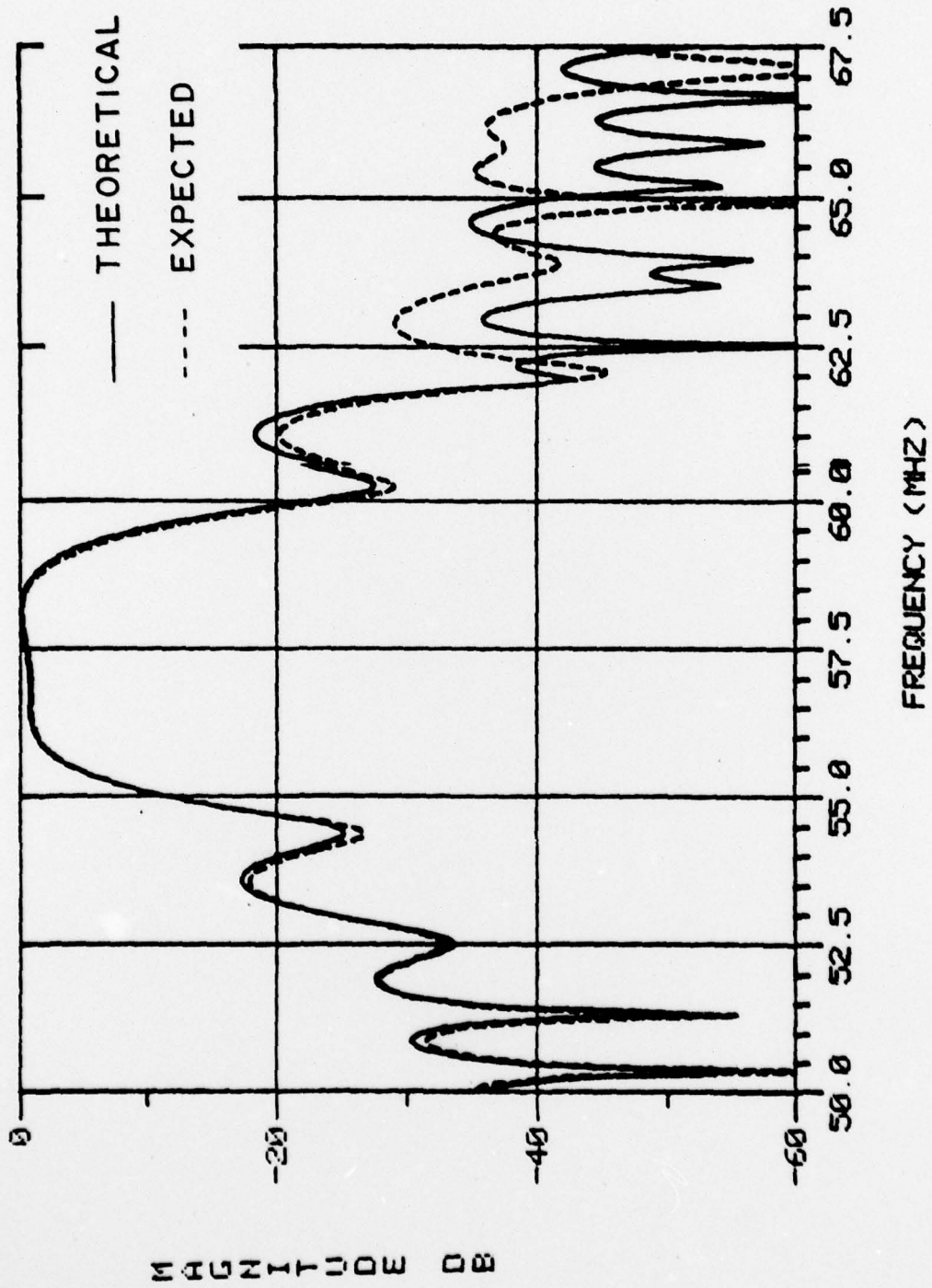


Figure 10a. Expected results device B, frequency response.

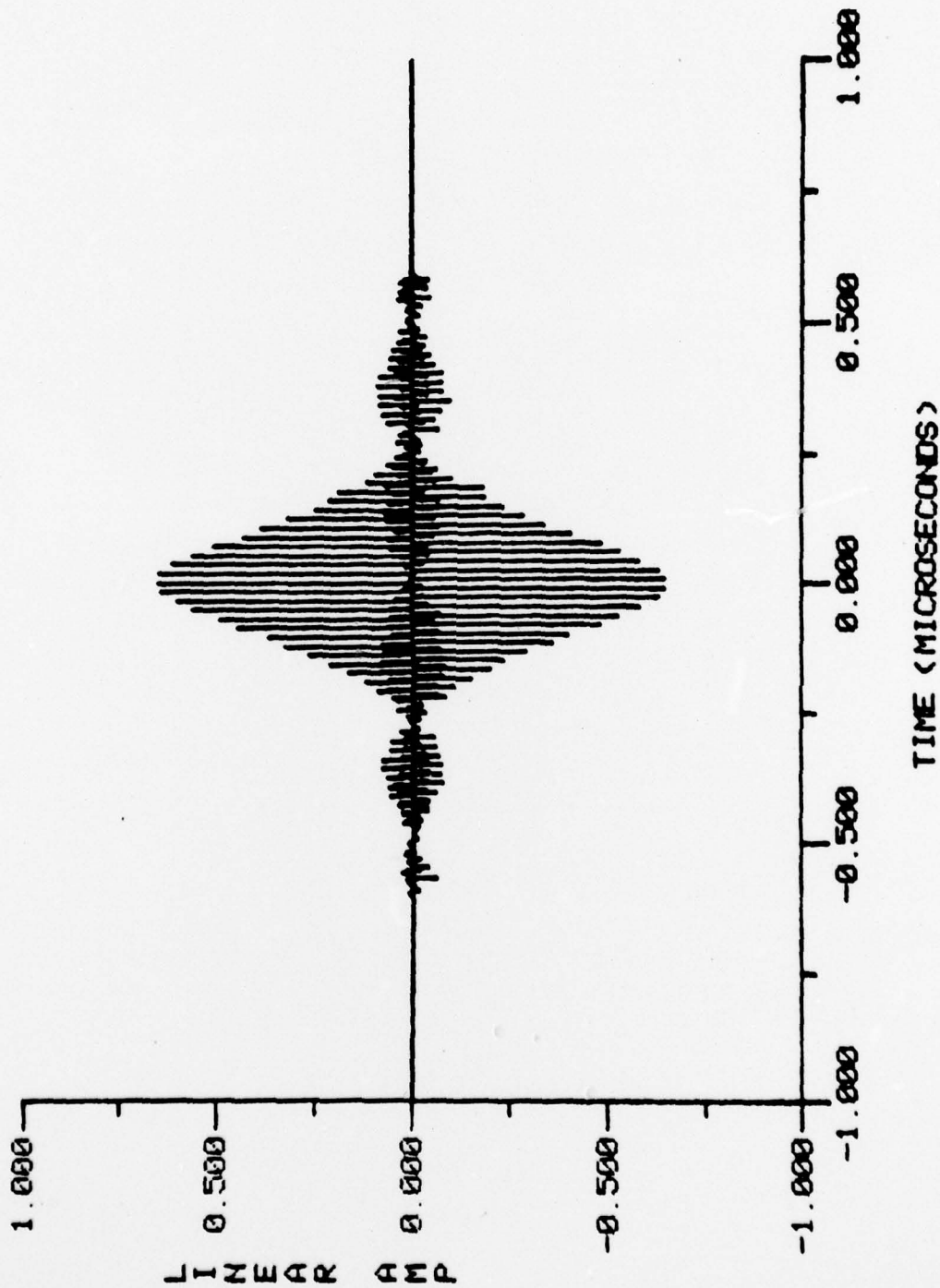


Figure 18b. Expected results device B, impulse response.

those of the specified response. Larger errors occur in the stop bands where the correction limit of figure 15 is dominant. These expected results assume that the amount of error in the original extracted error is much smaller than the original experimental error itself, that is the measurement-analysis process error is much smaller than the amount of error extracted.

VI. CONCLUSION

Surface Acoustic Wave filters are implemented in the time domain as the fourier transform of a specified frequency response. Correcting a transducer tap weight array involves the isolation from sources of error of an individual discrete impulse response where each sample is directly associated with an electrode. Since the discrete impulse response cannot be readily measured in the time domain because of the broad bandwidth involved, a set of frequency domain data is measured and then transformed into the time domain to provide the discrete impulse response of the overall transfer function. The sampling rate must be set precisely at four times the center frequency to accurately associate the discrete impulse response with the transducer elements. The output transducer tap weight and delay data is separated from the total response by deconvolution with the previously auto-deconvolved input-input response. The output transducer data now takes into account first-order plus all higher order isolated transducer responses such as regeneration, reflection, diffraction and bulk modes. The sampled data provides a convenient format for separating the transducer response from other modes in the time domain.

It is desired to extract the time domain error without regard to frequency scaling or magnitude scaling (insertion loss) induced errors. Two experimental output transducer discrete impulse responses from devices fabricated on the same substrate are compared with the theoretical tap weights and the resulting error responses are averaged. This consistent average error is used to pre-distort the

theoretical tap weights to produce a new set of tap weights which are designed to compensate for experimentally derived common additive errors. The expected experimental response is found by predistorting the already isolated output transducer responses.

Expected results are presented which show a marked improvement in frequency response accuracy with respect to the specified response. For the first time an experimental impulse response of an actual SAW device has been used to correct the entire transducer array in a straight forward manner.

APPENDIX

A. TETAM

The measurement equipment (figure 5) is buffered by an interface because each piece of equipment has different input-output requirements and they cannot be addressed in the serial format of the computer teletype line. The interface allows the selection of three modes: 1) present the six address characters to the synthesizer, 2) set the programmable attenuator and 3) read the meter values using three A/D converters. Each of these functions is addressed using a non-printable control character, so as not to clutter the terminal screen.

TETAM program operation is as follows. First, initial values such as sampling rate, percent of sampling bandwidth, FFT number, filename and center frequency are entered into the computer. The interface is sent a control character which bypasses the terminal and allows the interface to accept six characters which it sends in parallel to the synthesizer to address its various functions. Initially the synthesizer is programmed to the remote mode, the output is set at 0db and the starting frequency is entered. Second, the programmable attenuator is initially set to 60 db of attenuation using two characters, the first of which is a control character. The vector voltmeter is manually set to 60 db of gain giving an overall measurement system reference of 0db. A third control character starts the read sequence. The three 4 1/2 digit A/D converters sample the meter output voltages for 1 msec and after a 270 msec conversion time the values are present at the shift registers in the interface which

send them serially as nine characters to the computer. There the characters are converted to the three meter voltages which are scaled and combined to give the amplitude gain and phase shift across the device-amplifier combination.

The measurement system is designed for very accurate data acquisition with multiple constraints to be satisfied before a discrete frequency response data point is recorded. Before the synthesizer is commanded to step to the next frequency the program decides whether the vector voltmeter amplitude value is within meter range (0.2 to 1.0 volt). If there was no programmable attenuator and the amplitude range had been selected to not overload the meter during large passband values, the stopband values would be buried in the instrument noise (-50 db). Also at low channel B signal levels the vector voltmeter phase comparison circuit is unable to accurately operate. A programmable attenuator is used to change signal levels in order to optimize data accuracy. If the amplitude reading is too high (or too low) the programmable attenuator is incremented one step (10 db) up (or down), thereby automating the front panel vector voltmeter level range switch.

The vector voltmeter limits the accuracy and speed of the measurement system. Tests of the vector voltmeter search time have been made to optimize the reading sequence. The accuracy of the amplitude gain and phase shift across the device-amplifier combination limits the resolving power of the time domain analysis because the smallest time domain values are equal to the accuracy to which the frequency data was taken. The vector voltmeter uses a limited range

frequency sweep in conjunction with a phase lock loop to find and lock onto the frequency of interest. The meter was designed to follow a continuously varying frequency at a rate of 1 MHz sweep per second. In this application where the frequency synthesizer steps from one frequency to the next, the effective sweep rate approaches 100 MHz per second and the voltmeter briefly unlocks at each frequency change. Tests have shown that the phase lock loop has the least search time when the synthesizer frequency is stepped in an increasing manner. The average lock-in time is approximately 10 msec, but it is also possible for the vector voltmeter to unlock for no apparent reason at any time and for a random length of time. The combination of these factors precludes the use of an interface circuit which samples the vector voltmeter search (unlock) signal before allowing a read to occur. The command to read the meter values comes 10 msec after the frequency is changed in order to allow for the average 10 msec lock in time. The interface then samples the search line for 100 msec to allow all transients to die out. If the line has gone high during this period, the 100 msec sample restarts. If the line stays low, the A/D conversion is initiated. The vector voltmeter recorder outputs contain a 20 mv, 60 hz ripple (out of 1 volt dc max) which has been filtered with RC networks whose time constants are 30 msec. To further increase accuracy in critical sections of the frequency response (above -40 db insertion loss) two readings at a specified frequency are averaged.

B. MINERR

The minimum error program uses Newton's method to minimize the difference of the theoretical and experimental tap weights for two scaling factors. Magnitude scaling is deleted by weighting an experimental time domain data point by BETA and subtracting this product from the corresponding theoretical point. This error is then weighted by the theoretical time value and summed over the entire array. The theoretical weighting emphasizes the minimization of errors in the most important time regions. The sum of these theoretical weighted differences (WERR) is minimized by adjusting BETA, thereby producing an error file that has zero correlation with the theoretical.

$$\text{ERR} = \text{THEO} - \text{BETA} \times \text{EXP} \quad (\text{B-1})$$

$$\text{WERR} = \text{ERR} \times \text{THEO} \quad (\text{B-2})$$

The tests on frequency scaling error are carried out by frequency scaling the theoretical frequency response. This is done in the frequency domain by re-sampling the complex data using linear interpolation between data points. The previous minimum error steps are applied, only this time the weighted frequency scaling error is the absolute value of

$$\text{ERR} \times \text{THEO} \quad (\text{B-3})$$

where THEO has been frequency scaled. This essentially minimizes the "area" between the complex frequency responses. Finally the data is magnitude minimum errored giving an error file free of frequency and magnitude scaling factors.

C. APHAZ

The automatic time shifting program "straightens out" the frequency domain phase by subtracting a calculated phase slope and offset, thereby time shifting the data to time zero while maximizing the inphase component.

Initially the -3db points of the magnitude array are found. Over this range the phase array is fit with a least squares curve [8] producing the slope and offset values. The slope is simply the time delay and is subtracted out with the offset neglected. This process is continued until the slope is less than 1% of a delta t and then the offset is subtracted. Note, the phase is converted from modulo 2π to linear before processing.

D. AD

The auto-deconvolution program is used to extract the frequency response of a single input transducer. When two non-apodized impulse responses are convolved their frequency domain magnitudes are multiplied and phases summed. In the case of two identical non-apodized transducers a single frequency domain magnitude is squared while the phase is theoretically zero. The phase data is lost because the sinc(x) function phase is either zero or pi and when summed produces zero or 2π which after a modulo 2π operation results in a constant zero phase. To recover this phase information a

theoretical sinc(x) phase array is created and subtracted from the experimental phase array.

E. DECON

The deconvolution program separates the output transducer impulse response from the total device response by dividing the magnitude frequency domain arrays and subtracting the phase arrays.

$$\text{OUT} = \text{EXP} * \text{IN} \quad (\text{E-1})$$

The denominator array is magnitude normalized to keep the final data values within the original range.

REFERENCES

1. R.H. Tancrell, "Analytic Design of Surface Wave Bandpass Filters", IEEE Trans. on Sonics and Ultrasonics, Vol. SU-21, No. 1, January 1974.
2. C.S. Hartmann, D.T. Bell and R.C. Rosenfeld, "Impulse Model Design of Acoustic Surface-Wave Filters", IEEE Trans. on Microwave Theory and Technique, Vol. MTT-21, No. 4, April 1973.
3. C.M. Panasik and B.J. Hunsinger, "Precise Impulse Response Measurement of SAW Filters", IEEE Trans. on Sonics and Ultrasonics, Vol. SU-23, No. 4, July 1976.
4. A. Papoulis, The Fourier Integral and Its Applications, McGraw-Hill, New York, 1962, pp.120-131.
5. B.J. Hunsinger and R.J. Kansy, "SAW Filter Sampling Techniques", IEEE Trans. on Sonics and Ultrasonics, Vol. SU-22, No. 4, July 1975.
6. B.P. Lathi, Signals, Systems and Communication, Wiley, New York, 1965, pp.128-143.
7. E.O. Brigham, The Fast Fourier Transform, Prentice-Hall, New Jersey, 1974, pp.91-109.
8. C.F. Vasile, "A Numerical Fourier Transform Technique and Its Application to Acoustic-Surface-Wave Bandpass Filter Synthesis and Design", IEEE Trans. on Sonics and Ultrasonics, Vol. SU-21, No.1, January 1974.
9. C.F. Gerald, Applied Numerical Analysis, Addison-Wesley, Reading Massachusetts, 1970, pp.2-15.